University of Pardubice

Jan Perner Transport Faculty

Degradation Processes of Materials Due To Contact-Fatigue Loading

Utku KAYA

Dissertation Thesis

2016

Program of study:

P3710 Technique and Technology in Transport and Communications

Branch of study: Transport Means and Infrastructure

Supervisor: Prof. Ing. Eva Schmidová, Ph.D.

Dissertation came into being at department: Department of Mechanics, Materials and Machine Parts

I hereby confirm that:

I have written this dissertation thesis independently. All the reference literature and information used in this work are quoted in the list of reference literature.

I hereby acknowledge that all the rights and duties resulting from Act No. 121/2000 Coll., the Copyright Act, apply to my written work, especially that the University of Pardubice has the right to make a license agreement of use of this written work as a school work pursuant to to § 60 section 1 of the Copyright act. On the condition that the written work shall be used by me or a license shall be provided to another subject for the use hereof, the University of Pardubice shall have the right to require from me a relevant contribution to reimburse the costs incurred for the making of such work including all relevant costs and total overal expenditure and expenses incurred.

I agree with making the work accessible in the University Library.
Dated in Pardubice on 15. 6. 2016

Utku Kaya

I would like to express my special thanks to my supervisor: Prof. Ing. Eva Schmidová, Ph.D. for helpful approach, patience, and endless support. Words can never express how grateful I am. Her guidance helped me in all the time of research and writing of this thesis

ANNOTATION

Dissertation work is devoted to a problem with the determination of mechanical changes in surface layers of railway steels, induced by contact-fatigue loading. This study presents the current types of used rail steels and acting degradation mechanisms as a source of typical material degradation. The main problem for intended research is introduced on the base of the current restrictions for a description of processes acting in surface layers.

Used solution is based on application of the indentation methods for local mechanical properties measurement. Based on the experimental validation of standard methods, the work suggests the own attitude to direct comparative measurement. The Hadfield steel, including the explosive hardening effect, presented the experimental material. The comparison with the standard pearlitic steel endurance was based on rolling contact tests with defined longitudinal slip. Experimentally induced degradation effect was validated by structural analyses of operationally loaded parts for the both types of steels.

KEYWORDS

Contact fatigue testing, Hadfield steel, surface layer, deformation hardening, indentation tests

TITUL

Degradace materiálů vlivem kontaktně-únavového zatížení

ANOTACE

Disertační práce je věnována problematice hodnocení změn mechanických parametrů povrchových vrstev materiálů, indukovaných kontaktně-únavovým zatížením. Presentuje aktuálně používané typy kolejnicových ocelí a působící degradační mechanizmy jako zdroje jejich specifického provozního porušování. Hlavní řešený problém představují omezení pro standardní vyhodnocení uvedených procesů v tenkých povrchových vrstvách. Použité řešení je založeno na aplikaci indentačních metod pro měření lokálních mechanických vlastností. Práce vychází z experimentálního ověření zavedených metod a navrhuje vlastní přístup pro přímé srovnávací měření. Jako experimentální materiál sloužila Hadfieldova ocel se uvažováním vlivu zpevnění výbuchem. Srovnání odolnosti se standardní perlitickou ocelí bylo založeno na zkouškách kontaktně únavové odolnosti při definovaném podílu podélného skluzu.

Experimentálně vyvolaný degradační proces byl ověřen strukturními analýzami provozně zatížených materiálů obou typů.

KLÍČOVÁ SLOVA

Kontaktně-únavové zkoušky, Hadfieldova ocel, povrchové vrstvy, deformační zpevnění, indentační zkoušky

TABLE OF CONTENTS

LIST OF TABLES

LIST OF FIGURES

LIST OF ABBREVIATIONS

CYS	Comparative yield stress
HM	Martens hardness
hmax	Maximum indentation depth at Fmax
HM S	Martens hardness, determined from the slope of the increasing force/indentation depth curve
RCF	Rolling contact Fatigue
WEL	White etching Layer
Welast	Elastic reverse deformation work of indentation Nmm
Wplastic	Reverse deformation work of indentation Nmm
Wtotal	Total mechanical work of indentation Nmm
ηIT	Relation Welast /Wtotal

INTRODUCTION

Rail transportation is the way of transportation of passenger and goods by steel-wheeled vehicle. Railway transportation has big advantages such as the least affected by weather conditions, carrying extremely heavy goods, high-speed and cheaper transportation. Several types of steels have been used in railway. Using the same type of steel in every division of rail is a not efficient way because some part such as frog and switches encounter very high loading because of the dynamic load acting on the small surface on the tip of the frog results high wear as a result of the rail vehicle hits. Because of that, Switches and crossing have specific design and reliable materials to prevent abrasive wear and fatigue. In this thesis, we will start with a brief introduction about rail-wheel contact mechanism. As a result of high loading, wear and defects types will be mentioned. Pearlitic, bainitic and Hadfield steel which is used commonly in railway grades will be defined.

The operational loading of the rail´s material is very complicated, the aim of this study is understanding degradation mechanism and mechanical behavior of railway materials under operational and experimental loading. From the point of subjected materials, the evaluation will focus on Hadfield steel compared to standard pearlitic steel of the R260 grade.

Several experiments were applied to define mechanical behavior of Hadfield and pearlitic steel grades. The experimental methodology consists; after simulation of rolling contact process by rolling stand wear resistant was examined, metallographic analyses were applied to investigate surface and subsurface layers, and standard hardness measurements were used to evaluate the intensity and depth of hardening .Examination of limited surface degradation was tested with Vickers, cylindrical and spherical indentation method. Type of indenter was chosen according to their capabilities. Indentation methods and indenter types will be compared and new mathematical approaches for the testing method will be introduced.

The rolling contact fatigue (RCF) resistance of Hadfield steel was tested in two states, with and without explosive hardening. Experimental loading was adjusted to the real operational ratio between the normal loading and longitudinal slip. Strengthening effect of the surface layer was monitored at chosen loading stages and verification of experimentally induced degradation process was based on structural analyses of the operational induced process. Instrumented

indentation test was employed for evaluation of elastic-plastic capacity under the influence of hardening in compared states of Hadfield steel. Operational, experimental loaded with and without explosive hardened samples are compared and examined with several types of hardness measurements.

1 RAIL-WHEEL CONTACT MECHANISM

Demands of heavier axle load, higher speeds, and more comfortable transportation are increasing, because of that understanding rail-wheel contact mechanism has an important role in improving new rail vehicle and optimize rail design. The performance of rail vehicle depends on very small contact areas between real and wheel. Typical rail and wheel design can be seen in figure 1. This design purpose to absorb vertical and lateral and horizontal forces. Durability against drive force provides comfortable transportation and prevent derailment

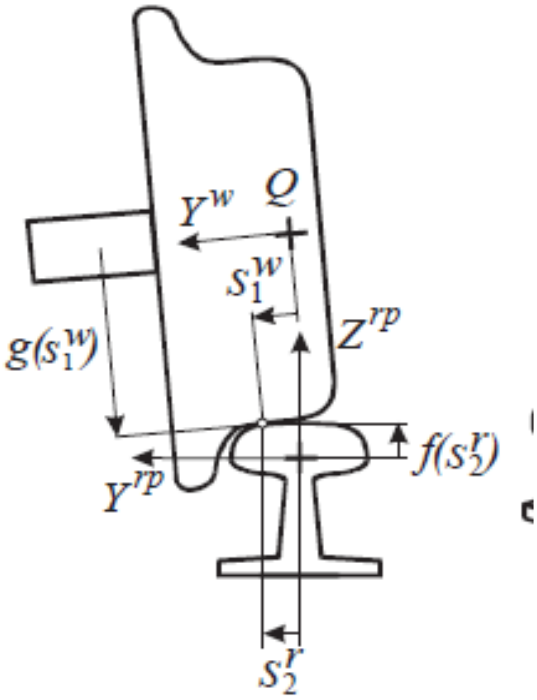

Figure 1 Typical rail and wheel design [1]

Rail wheel contact mechanism divided into two parts; geometric and elastic part. The geometric part is related with kinematical data of wheelset such as; wheel-rail shapes, track geometry and irregularities in track but the elastic problem is commonly finding contact area , contact pressure and creep force in wheel-rail contact. Geometrical part is initial approximation to start for elastic problem.

Rolling contact mechanism has been studied many investigators such as Carter, Johnson and Kalker[2],[3],[4] .Their theory lets us calculate rolling contact mechanism and implement by FEM analysis. Development of FEM analysis for rolling contact started in the early 1980's [5]. Besides that, Heinrich Hertz solved contact problem of two elastic bodies with curved surfaces [6] and his solution is still used for modern contact mechanism.

Rail-wheel contact phenomenon has been widely investigated and still important for the studying of the dynamic behavior of a railway vehicle. Providing low energy usage, less noise, and comfortable vehicles depend on adhesion level between rail and wheel. Adhesion is the force required to separate two surfaces that have been brought into contact and describes how surfaces bond each other. However, the term "adhesion" is defined as the tangential force between wheel–rail contacts as used by et al. Fletcher et al. [7] and Lewis [8].

Adhesion is an important factor to provide tracking. Adhesion force between the wheel and rail often decreases due to the lubricating because of water film during raining and snowing. If adhesion force is smaller than wheel driving force, wheels slide during accelerating and braking. This slipping and sliding will result in high energy usage and damage in rails because of that it is important to consider adhesion mechanism and taking precaution for undesirable effects.

Demands of acceleration and braking are increasing. Shorter braking distance and higher acceleration are important for improving transportation time. The friction between rail and wheel has strong influence about breaking and acceleration time. In another word, if friction is low, the train cannot be able to break within available distance. Increasing friction solves this problem but high friction result wear and maintenance cost. Snow, rain, high humidity and leaves in autumn results lubricant layer which consists fallen leaves (so- called black layer), water, rust, etc. between wheel and rail. This layer results decreasing in friction. Low friction results in big economic issues such as wasting energy usage. Beside that driver take big responsibly because of weak breaking. Thus, finding an optimum level between friction coefficients and preventing wear is still research subject.

To overcome these issues, the sand is often mixed with metal particles and is delivered by a gel paste, the final mixture being referred as "Sandite" [9]. Sanding is one method of reducing wheel slide. Locomotives have sandboxes which can deliver sand or sandite to the rails in front

of the wheels .Other proactive solutions include cleaning the rail by, for example, high-pressure water jetting as seen figure 2 [10].

Figure 2 Water jetting to prevent slide [10].

There is also another method to prevent sliding, such as Wheel Slide Protection (WSP) equipment which is generally fitted to passenger trains to manage the behavior of wheel sets in "low adhesion" (reduced wheel/rail friction) conditions. This system is similar anti-lock braking (ABS) for car and controlled by programmed microprocessor

Friction in dry contacts takes place at the micro level and is generated in the microcontacts of surface roughness. In the simple (not reality) system the coefficient of friction is often referred to as Coulomb type. In real operational loading is Coulomb type anymore and it is more complex mechanism which is divided by adhesion and slip as seen in figure 3

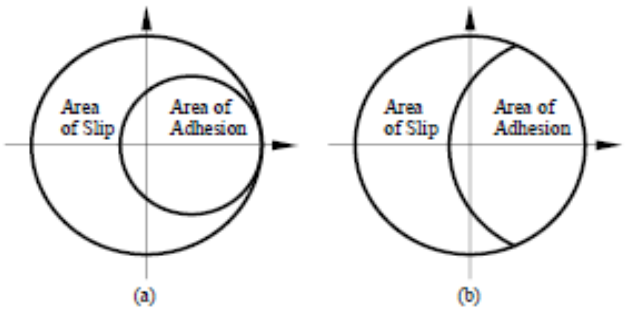

Figure 3 In operational loading contact area divided into adhesion and slip [11]

The pure rolling motion doesn't exist in proper adhesion level. In fact, there is always small sliding between rail and wheel in operational condition. This phenomenon has been described as pseudo sliding or micro creepage. Carter performed an experiment on steam locomotives in 1930.

This study showed the speed of the wheel is not the equal speed of the vehicle. In another word, there is no pure rolling contact. The increasing traction torque results to perfect adhesion to full slide condition. This was the first proof of creepage. Creep in rail is defined as the longitudinal movement of the rails in the track in the direction of motion of locomotives. There is a big relation between adhesion coefficient and creep.

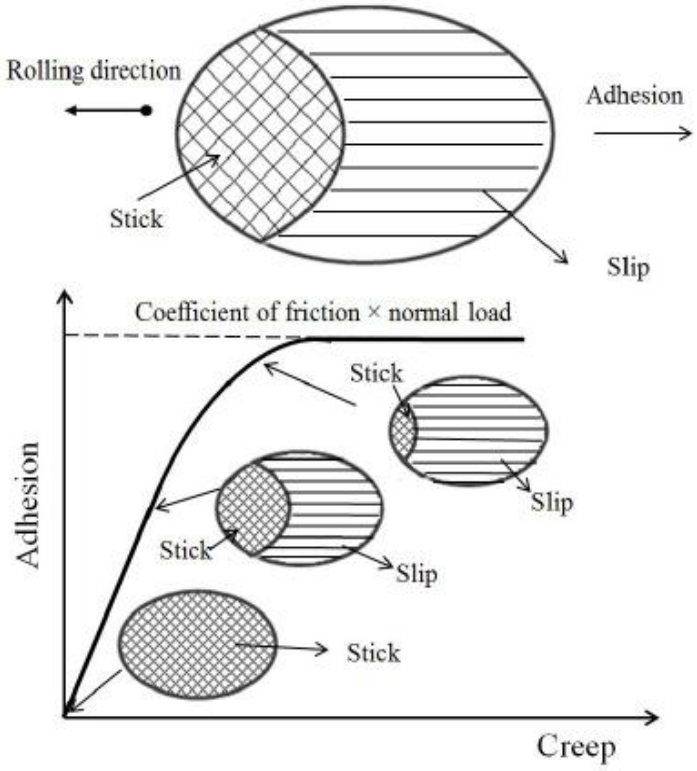

Figure 4 Creep curve [1].

Creep curve can help to detail slip mechanism of wheels during braking and accelerating. It can be seen in figure 4.When the creep is zero, the whole contact area sticks and known as "effective slip". However, zero creep does not exist in reality. Slip occurs at the trailing edge and spreads forward through to the contact area as the adhesion increases. The slip region increases and the stick region decreases resulting in a rolling–sliding contact until pure sliding appears. In that state, the adhesion equals the friction force between two bodies under pure sliding conditions [1].

2. IDENTIFICATION OF MATERIALS PARAMETERS DISTINCTIVE FOR OPERATIONAL DURABILITY

2.1 A specifics of the material response to the rolling contact loading

Rails are an important part of the railway infrastructure. The quality of rails has directly affect railway transport. Increasing speed, improving heavier axle load depend on rail design.Solid rail always needs to have suitable mechanical behavior such as wear resistance, thermal crack resistance, strength, anti-rolling contact fatigue and good vibration characteristic. Besides that, rail needs to have special design to tolerate vertical and lateral forces,

Rails consist of several parts which are highly affected by wear and loads . Frog switches encounter very high forces. Typical frog design can be seen figure 5. Several measurements shows, biggest wear occurs in frog switches. The dynamic load acting on the small surface on the tip of the frog results in high wear as a result of the rail vehicle hits. Because of that, switches and crossing have specific design and reliable materials to prevent abrasive wear and fatigue.

Figure 5 Typical frog switch

Many service failures occur from the growth of cracks subjected to mixed mode loadings. During rail-wheel contact, several modes of vibrations occur. Shallows and ununiformed rail grades accumulate magnitude of modes. As a consequence, the crack tip of a head check or squat experiences a moderate initial mode I cycle followed by a mode II shear cycle, at the end of the cycle, additional mode III loading can occur. Such a sequence is illustrated in figure 6. Small magnitude mode such mode I is not responsible for rail cracks.

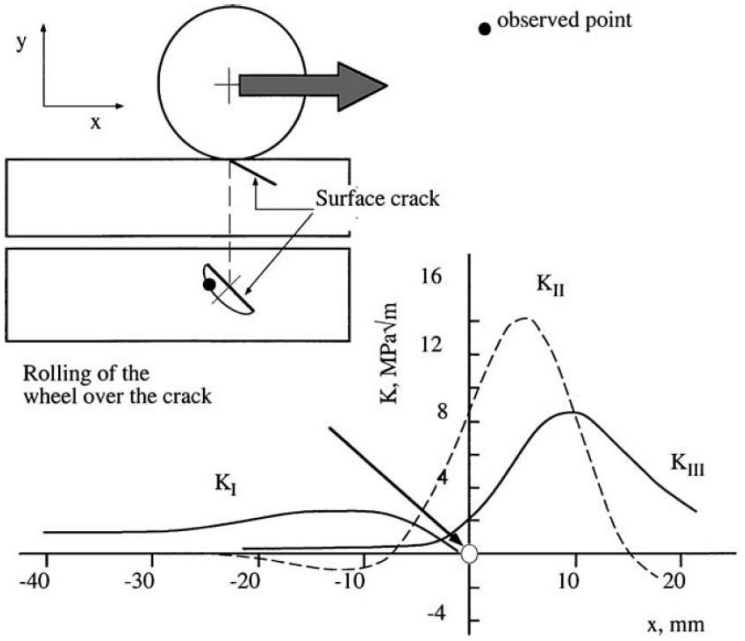

Figure 6 Mixed mode loading sequence a rail is subjected to during wheel pass over [12].

Rest of rail infrastructure suffers from wear as weel as Frog switches. During operational loading, high surface stress occurs in the elliptic area between rail and wheel. Besides that rail surface is subjected to rolling and sliding and relatively high contact stresses. This type of stress results major plastic deformation in the surface area of rail in case of yield strength (plastic shakedown limit) of rail exceed. In other words, Ratcheting occurs under the cycle of loading. Although the plastic deformation due to Cycle loading may be very small, the plastic deformation accumulates to large values over many cycles of loading. This can be seen in figure 7. When the ratcheting exceeds ductility limit of the surface, crack initiated from the surface, these may subsequently lead to flaking or spalling. To prevent this occurring, the cracks can be removed through grinding .Ratcheting plays an important role in rolling contact fatigue. Because of that, it is essential to improve rail design to prevent ratcheting.

The rail carries the massive dynamic load. Repeating load in a vertical and tangential way increase internal cyclic stress which damage the material and also result of initial small cracks that will initiate from rail surface before propagating horizontally even in some case vertically which cause rail break, and a serious accident. Cyclic stresses and the plastic deformation are the major factors influencing the rail degradation processes [13, 14].

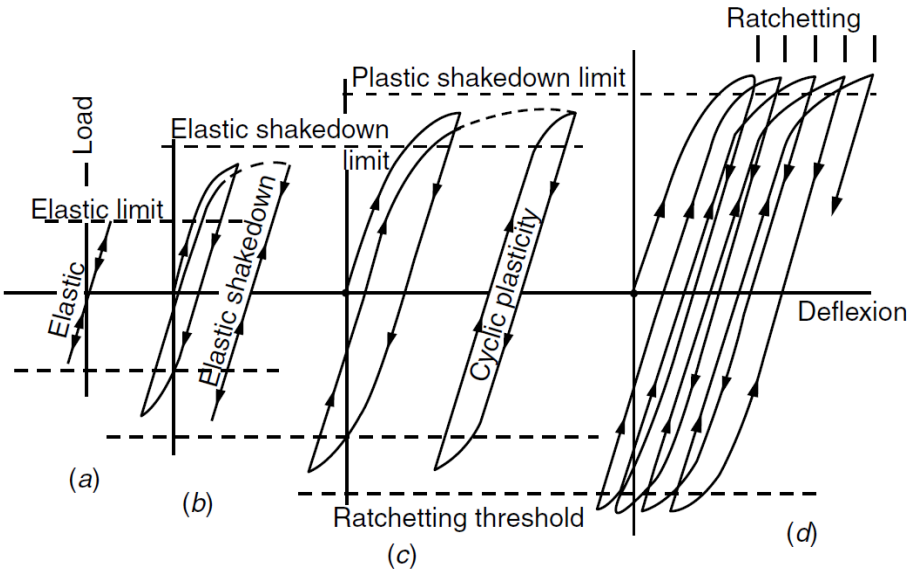

Figure 7 Response of material to repeated (cyclic) loading [15].

The stages of the development of the cracks can be decomposed into separate phases as shown in figure 7. [15]

1. The perfectly elastic response is wholly elastic after the initial transient response (Figure 7a).
2. Elastic shakedown plastic deformation can be seen in early stages but, due to the development of residual stresses and sometimes strain hardening, the steady-state behavior remains perfectly elastic (Figure 7b).
3. Plastic shakedown, there is no obvious plastic deformation but reverse plasticity occurs leading to low cycle fatigue. This behavior is sometimes referred to as cyclic plasticity (Figure 7c), and the corresponding limit is called the plastic shakedown limit or the ratcheting threshold.
4. Above the ratcheting threshold, the plastic strain increases with every load cycle until rail breaking (Figure 7d),

Ductility is exhausted above ratcheting threshold and inclined cracks are formed under the surface and initiate rapidly.

Characteristic required for rail analyses

1. Fatigue strength : Rail should withstand several cyclic mechanical stress during operational loading
2. Fracture mechanics: The initiation phase of a fatigue crack and a microstructural crack extension phase should be determined.
3. Rolling contact fatigue(RCF) strength: RCF starts with small initial cracks. Rail should withstand high loading in small contact area
4. Thermal stress and thermal cracks : During acceleration and breaking , the extremely high temperature can transform rail surface another material form. This form cannot withstand wear and RCF
5. Wear resistance : Wear always exists for all materials. Friction between wheel and rail results abrasive wear. The level of wear increases during accelerating and braking.
6. Bending skills : specific part of rail should be elastic (flexible) to absorb lateral and vertical force and steel should be characterized by high-level endurance and hardness and good resistance to abrasive wear as well as lower ductility and crack resistance
7. Price : Railway steels are extremely expensive materials (Especially maintenance cost). Designer should consider cost parameters because of that it is important to develop rail with low-cost material and highly resistant against environmental condition

To observe characteristic: Rail design should provide requirement above. There are several examinations and testing method.

The prescribed qualifying examination is the following:

- fracture toughness
- fatigue crack growth rate
- fatigue testing
- residual stress in rail foot
- tensile strength and elongation

Acceptance tests

- microstructure
- the degree of decarburizing charred layer
- the purity of steel
- macrostructure
- hardness
- tensile strength

2.2 Wear mechanism of railway materials

Wear is the phenomenon of material removal from a surface due to interaction with another surface. It is the result of material removal by physical, chemical dissolution, or melting at the contact interface. Wear occurs almost all machines lose their lifetime and reliability due to wear, and the possibilities of improving new advanced machines are reduced because of wear problems. Because wear mechanism should be taken into consideration to improve new reliable machines. Wear mechanism is not a simple and single mechanism. There are several types of wear as adhesive, abrasive, fatigue, and corrosive. All of this wear types can be seen in rail grade. Wear due to environmental effect should be taken into consideration because of passenger.

2.2.1 Adhesive wear

Adhesive wear is a phenomenon which occurs when two metals rub together with sufficient force to cause the removal of material from the less wear-resistant surface. When two surfaces come in contact, the strong adhesive bond is formed at the tip of the asperities and consequently, adhesive wear particle is formed by shearing the interface caused by sliding.
According to the theory of Hertz, the contact area between rail and wheel is an ellipse form. Wheels roll over the rail as a consequence of dry friction, the bodies can apply tangential forces upon each other at the contact area. The tangential force in the longitudinal direction during both acceleration and deceleration is referred to as adhesion. The ratio between the adhesion force and the normal force is known as the adhesion coefficient. Creep in rail is defined as the longitudinal movement of the rails in the track in the direction of motion of locomotives

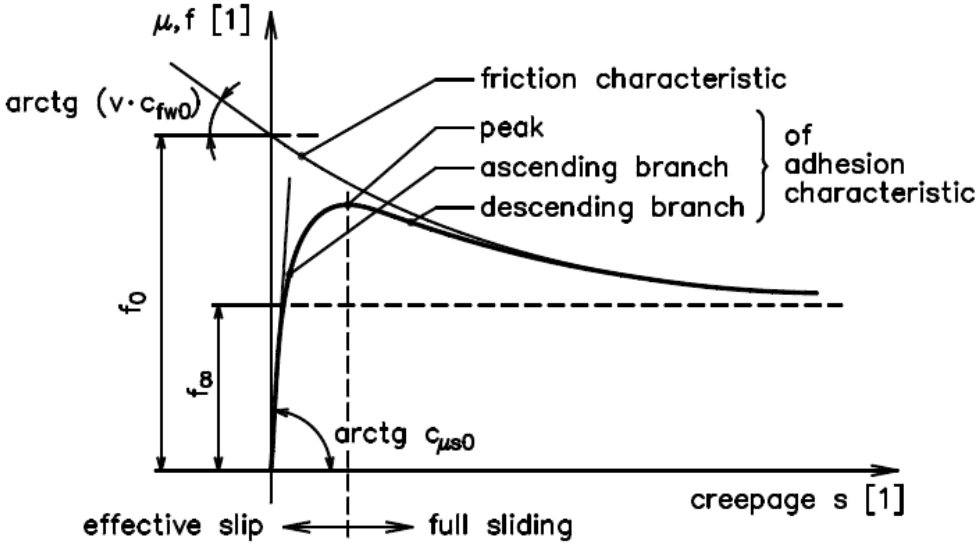

Figure 8 A sketch of the theoretical friction and adhesion characteristics [16].

Creep curve can help to detail slip mechanism of wheels during braking and accelerating. It can be seen in Figure 8. When the creep is zero, the whole contact area sticks and known as "effective slip". However, zero creep does not exist in reality

2.2.2 Abrasive wear

Abrasive wear occurs due to the indentation of the hard surface into the soft surface. This result ploughing instead of sliding process. As a result of ploughing volume of the surface is removed. For example, sanding is used in train operation to improve adhesion at the wheel/rail interface during both braking and traction. Sanding also leads to progress of abrasive wearing. In figure 8 abrasive wearing between rail and wheel as a result of sanding.

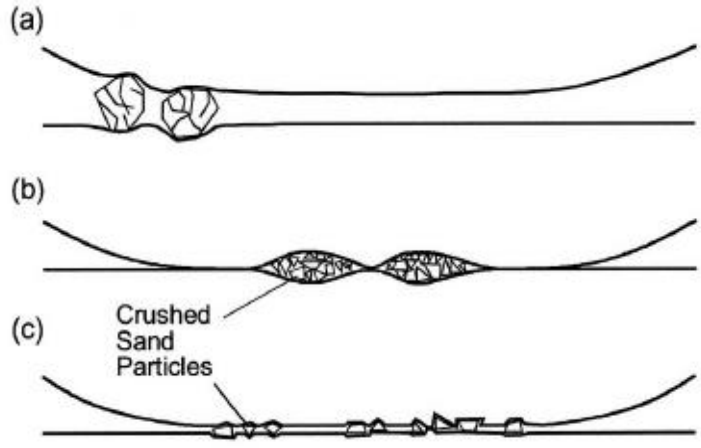

Figure 9 Example of abrasive wearing due to sanding [17].

2.2.3 Fatigue wear

Rail wheel contact with very high local stress are repeated a large number of times during sliding or rolling; High plastic deformation causes crack initiation, crack growth, and fracture. Fatigue wear occurs when shear stresses or strains between rail and wheel exceed the fatigue limit for one of surface material.

2.2.4 Corrosive wear

Corrosive wear occurs when the contact surface chemically reacts with the environment and form new layers. This layer has different strength than real material. And this layers in surface removed by mechanically as mentioned above.

2.2.5 Rolling contact Fatigue

Rolling contact fatigue (RCF) is a common problem for all types of railway which resulted in wheel damages and reduced the lifetime of the wheels and in the worst case derailment of the train. Replacing rails and wheels is very expensive, because of that, it is important to produce the rails and wheels more wear resistant. Controlling rolling contact fatigue has big importance improving faster, cheaper and reliable transportation. Stress and slip are the main reason of RCF. Before the introduction of railway defects, the definition of White etching layers will be introduced. RCF will be explained more detail in next chapter.

2.2.6 White Etching Layers in Railway steel

WEL (White etching layers) is one of the defects in rails. In order to observe this layer, the prepared surface has to be etched than observed by optical microscope. After etching process, it is possible to see the white area as seen by light microscopy near the surface. There are two ideas about the reason of WEL. During accelerating and braking raises the temperature enough to transform the steel to austenite and subsequently cooled fast enough to result in martensite. The other possibility is, repeated contact breaks down the microstructure.

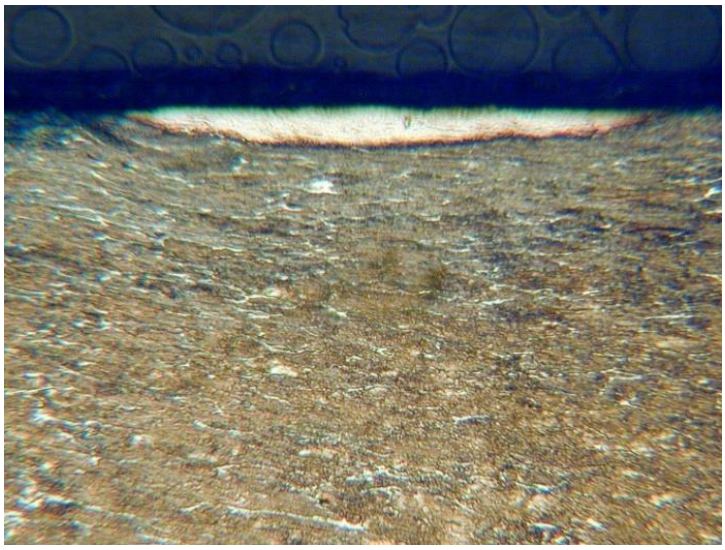

Figure 10 Creation of the WEL in pearlitic rail steel

"White Etching Layers" (WEL) is one of the mechanisms of surface microcracks initialization were involved in the wear during the rolling contact and typically formed in pearlitic railway steels. This name was derived from its white appearance, resulting from its higher corrosion resistance against metallographic etching. Contrast phase was created by simulated contact fatigue up to a depth of 30µm, typical was a different level of plastic deformation inside these layers. The voids and microcracks are created directly in this layer approximately perpendicularly to the contact surface, apparently as a consequence of fragility of these micro volumes as in figure 10.

2.3 Defects in rails

It was already explained reasons of defects, rolling contact fatigue and ratcheting mechanism. The durability of rails is determined by wear , plastic flow, and defects.

Wear : wear always occurs on the gauge face. There are many ways to decrease wear but there is no way to eliminate.

Plastic flow: Plastic flow occurs due to high loading exceed yield strength of material

Defects : Defect can occur by plastic flow and wear. İt is important to detect in time. Otherwise, it will result in brakes and derailment

Some of the defects are in rail grades

- Waves
- Rolling contact fatigue
- Squats defects
- Oval or Shatter cracking
- Vertical Split head
- Horizontal split head
- Wheel burns

There are several defects in rails. We will introduce 3 different defects commonly seen rail. Most importantly, rolling contact fatigue will be investigated in this thesis and introduced with several experimental output.

Defects in rail (all of the photos are taken from **Ceske Drahy CD s 67** standards)

2.3.1 Waves

This defect is caused by the longitudinal sliding action, acceleration, braking or lateral motion across the rail. Higher nominal loading , higher vehicle speeds, smaller wheel radius and higher friction between wheel and rail increase the tendency to this defect creation. This deffect can be seen in figure 11.

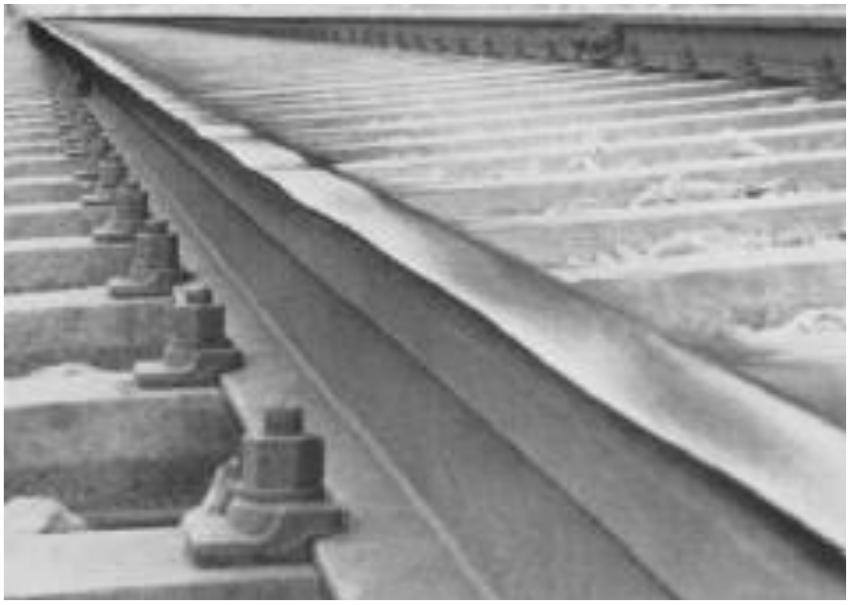

Figure 11 Waves defect [CD s 67]

2.3.2 Rolling contact fatigue

In this thesis, we will commonly focus on rolling contact fatigue. Experimental procedure and analysis will be introduced and reason of rolling contact fatigue will be analyzed . RCF occurs the gauge corner zone .Type of rolling contact fatigues;

Gauge corner checking (Head checking)

This defect occurs mainly in the gauge corner region of the high rails sharper curve The gauge corner checking crack are initiated very close the rail surface. This crack looks like very small lines on the surface as seen figure 12

Figure 12 Gauge corner checking [CD s 67]

Sheeling

This defect initiates on gauge corner and may result in crack. These defects do not regularly along the rail gauge as gauge corner checking and commonly looks like black spots. This effect can be seen figure 13.

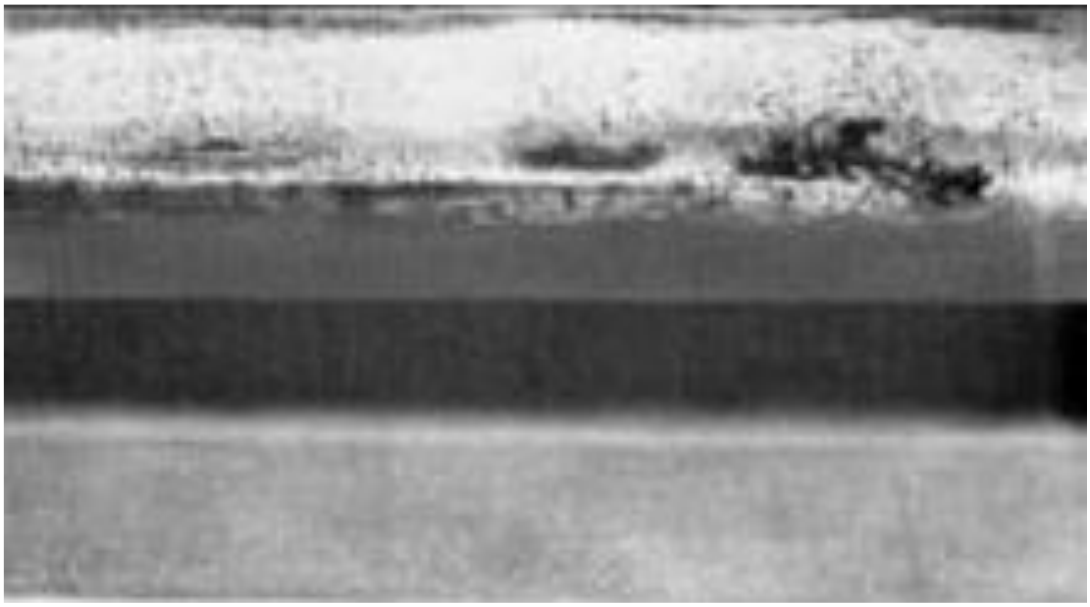

Figure 13 Sheeling [CD s 67]

2.3.3 Squats

Squats can initiate at small indentations, corrugations, and welds and commonly looks like figure 14 .It is important to detect squats at an early stage to keep degradation in minor level , the cracks can be easily treated by light grinding a from the surface.

Squats are commonly initiated at a rail head or gauge corner checking tracks. Each squat results in sub- surface cracks which propagates in travel direction and opposite direction as seen figure 15. Squats which are initiated from gauge can be the same category as rolling contact fatigue.

However, recent works show that squats from rail head are initiated often because of white etching layer phenomenon. Squats are important problem which results that rail life is decreased because of that need for aggressive and expensive defect grinding

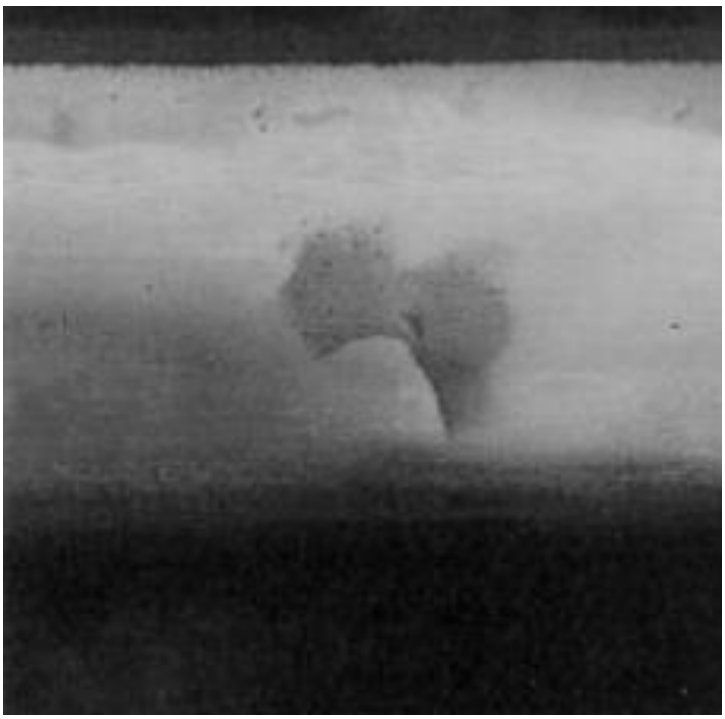

Figure 14 Squat defects [CD s 67]

Figure 15 Squats results sub- surface cracks which propagates in travel direction and opposite direction [CD s 67]

3 RAILWAY STEELS

A basic grade of steel used for the production of rails and sections for railroad switches is carbon-manganese steel with a pearlitic structure. Pearlitic rail steels display lower susceptibility to ratcheting. Their hardness varies in a wide range from 200 to 390 HB. Pearlitic steels should be characterized by high-level endurance and hardness and good resistance to abrasive wear as well as lower ductility and crack resistance. Pearlitic steel resistance can be increased by amount modification such as heat treatment and isothermal annealing.

One alternative pursued in recent years is the use of bainitic rail steels. In conjunction with the appropriate alloying additions and, if need be, a suitable form of heat treatment, these can attain sometimes greater strengths than pearlitic steels. Besides that, Hadfield steel has been used for switches and crossing because of its resistance under extreme load.

3.1 Pearlitic steels

Pearlitic steels have been used for a long time and it still a major part of all railway rail steels. Pearlitic steel consists ferrite and cementite phase. Pearlitic steel is obtained when austenite for is heated above 727°C. When austenitic steel is cooled its equilibrium reaction to cooling is to transform to ferrite. Since ferrite can solve only very small amounts of carbon, a

second phase is created, cementite, which has high carbon content. Pearlite is a two-phased, lamellar (or layered) structure composed of alternating layers of alpha-ferrite (88 %) and cementite (12 %) that occurs in some steels and cast irons. The pearlitic steel structure is shown in figure 16.

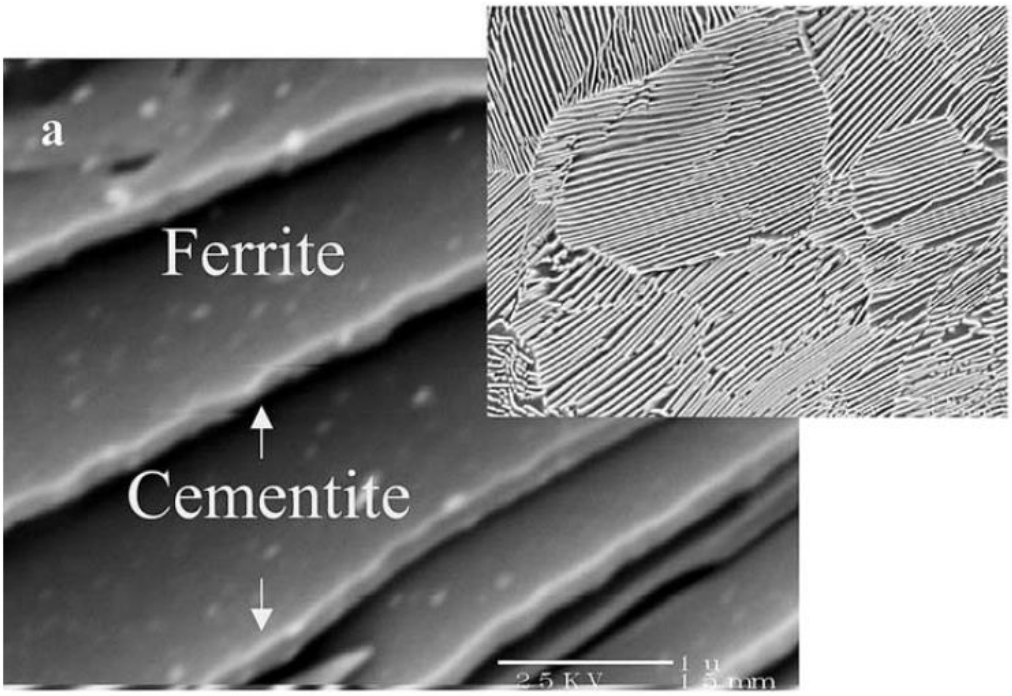

Figure 16 Microstructure of pearlitic steel [18]

The demand of railroad industry increases. More than 40-ton axle loads are still using because of that wear rate of rail steels should be considered. In figure 17, the relation between increasing contact pressure and wear rate can be seen.

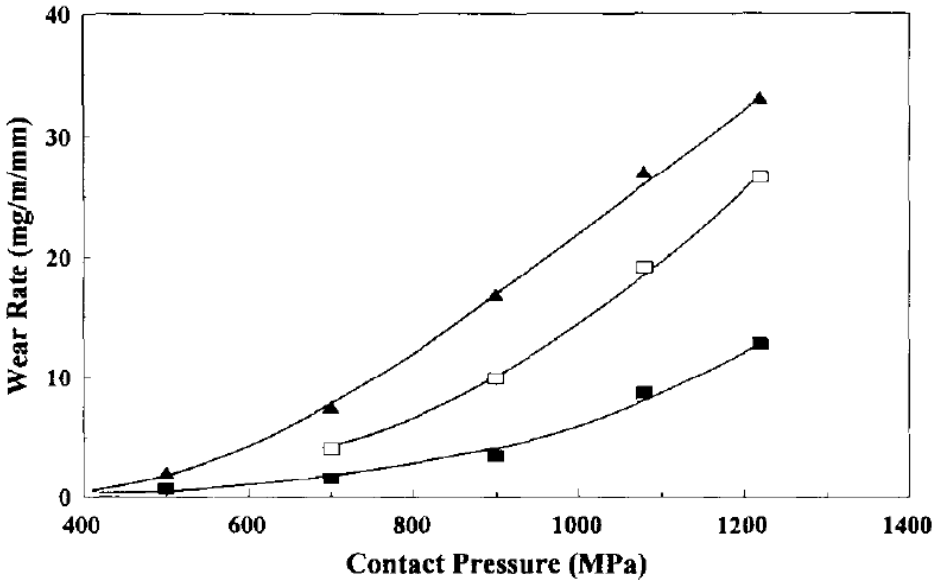

Figure 17 Non-linear wear rate vs. contact pressure curves [19]

The amount of ferrite and cementite layers give pearlitic steel's mechanical properties. Some layers are harder and brittle cementite rest of them are softer and ductile ferrite. Characteristic of this layers can be changed by carbon rate. In other words, carbon and cooling rate specify mechanical properties of pearlitic steel. There are some methods to control mechanical properties of pearlitic steel. One way is using alloy elements which are a costly method. Another way is controlling production process and avoiding unwanted carbides, sulphates, and intermetallic particles. In addition, cooling rate forms the thickness of the cementite and ferrite layers. This thickness can be measured average distance between two layers which named as inter- lamellar distance.

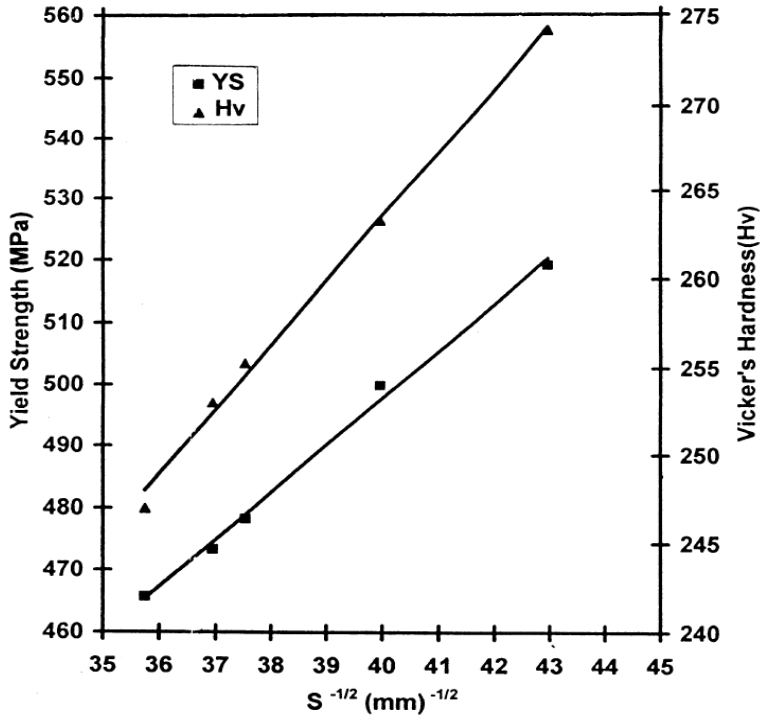

Figure 18 The hardness and yield strength as a function of the inverse of the square root of the interlamellar spacing [20]

The mechanical properties pearlitic steel is under influence interlamellar spacing. Thermal treatment results in size reduction of pearlite colonies and a reduction of the interlamellar distance in cementite. In consequence, the properties of a Pearlitic rail steel and the durability of rail sections change [21]. The steel had been heat-treated at different austenitization temperatures in order to observe interlamellar spacing's role. The hardness and the yield strength of the steel samples are plotted as functions of the inverse of the square root of the interlamellar spacing both hardness and yield strength follow a linear relationship with $S^{-1/2}$ [20]. (in figure 18)The Same type of result also obtained in another investigation [22].

3.2 Bainitic steels

Bainitic steel can be produced by slowly cooling austenitic form above 730°C. It is possible to produce different quality Bainitic steel according to cooling rate. Bainite with carbides along the ferrite components is known as upper bainite at a high temperature of the transformation range. At low temperatures, it appears as a black needle-like structure resembling

martensite and is known as lower bainite. Upper and lower bainite have a different type of mechanical properties. When cooling process at a temperature of between 550° to 400°, cementite layers tend to lie parallel to ferrite layer as a needle shape which named as upper bainite, lower Bainitic steel is produced at a temperature cooling level of 400° to 250° Celsius and carbide be formed within the ferrite needle which is transversely at an angle of 55Â° . For example, upper and lower bainite structures can be seen CrMnSiMo alloy cooled at 33 °C/min in figure 19 [23].

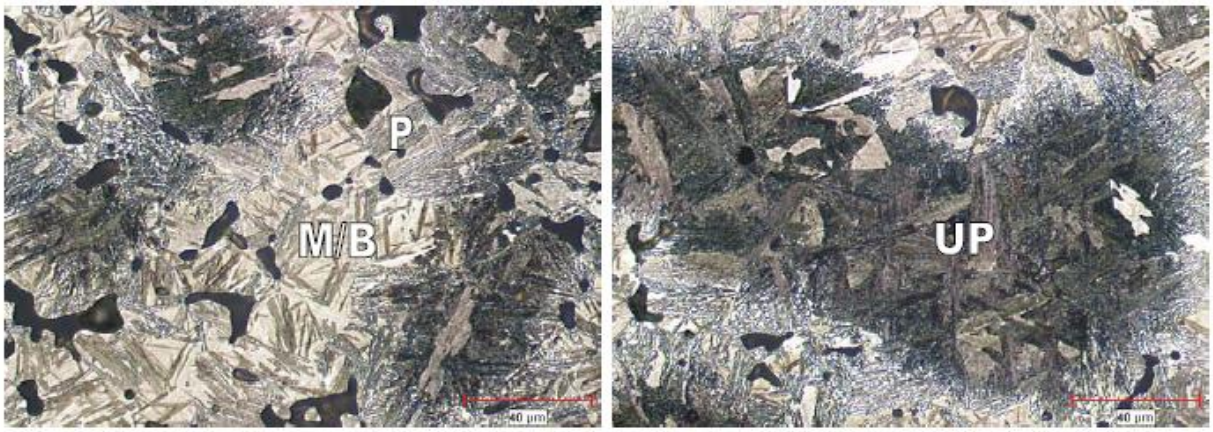

Figure 19 Microstructures of the CrMnSiMo alloy cooled at 33 °C/min. Martensite (M), lower bainite (B), pearlite (P) and unresolved pearlite / upper bainite (UP) are present [23].

Carbide free type bainite steel is used for railway applications. The wear behavior of Bainitic steels under rolling and sliding conditions has been studied for several circumstances [20–22]. According to some experimental work, some of the Bainitic steel structure obtain dry sliding wear resistance as wear-resistant Pearlitic steels. Besides this, over the hardness range 230 - 300 HV 30, the wear resistance of the low carbon Bainitic steels was comparable with that of high carbon Pearlitic steel [23]. Bainite rail grades which include no carbide can be harder than Pearlitic rail grades. Because of that, it has been used for switches and crossings. But the main problem about Bainitic still is hard to predict its performance before production. Because of that Bainitic steels are still research subject.

3.3 Austenitic steel with high manganese content (Hadfield steel)

The austenitic Hadfield steels, containing about 1.0–1.2 mass% C and 11–14 mass% Mn, and originally proposed by Hadfield (1925), have excellent wear resistance property. Above

730°C steel has austenitic structure form. When the temperature drops, this structure transforms different structure like Pearlitic steel .To produce austenitic steel is needed to use elements that prevent transformation to other forms. Manganese is one of them. For example Hadfield steel as seen in figure 20 is the type of austenitic steel which has around 13 wt% of manganese.

Switches and crossings when wheels have to pass from one rail to another, impact loads are very high. For these situations, it is necessary to use extremely resistant against wear and another environmental condition. Hadfield steel is a good choice for this kind of situations. Hadfield steel is high resistant against wear because of that it is used in stonebreakers, bulldozer blade edge, and high load railway applications. However, the Hadfield steel often has poor performance when the impact energy is not high enough to achieve a notable work-hardening result [27].

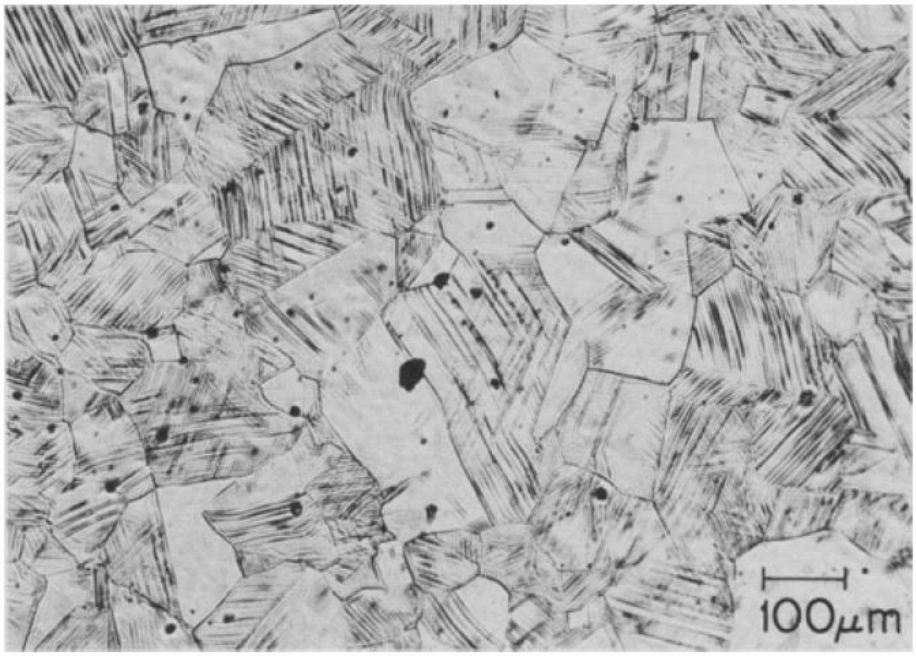

Figure 20 Microstructure of high manganese austenitic rail steel [28].

3.3.1 Effect of explosion hardening in Hadfield steel crossing

Austenitic manganese steel, known as Hadfield steel, is specially employed for the casting of railway crossings, because of exceptional work hardening capacity and fracture toughness, proved by some experimental works [29, 30] Depending on the loading conditions, a rapid

deterioration of parts can occur if wear is faster than work hardening. Explosive hardening is, therefore prospective way to improve the service life [30].

The explosion hardening technique can increase the hardness of metals by severe plastic deformation caused by the shock wave. Norman first reported an explosion hardening technique in 1955 and got a patent for this technique [31]. The hardening impact wave is induced by the detonation of the charge which is attached metal component surface as seen figure 21. Semtex 10SE (producer Explosia Pardubice) explosive material was introduced crossing materials. It is one of few methods to make materials gaining higher strength and higher hardness. This method can be used Hadfield steel, pertinently some other metals, carbon steels, stainless steels and copper as well.

Figure 21 The charge application on the crossing running surface [32].

Explosive hardening results dislocations which can be observed by a microscopic scale dislocation is capable of traveling throughout the lattice when relatively small stresses are

applied. Increasing the dislocation density increases the yield strength which results in a higher shear stress required to move the dislocations. This results in resistance to plastic deformation.

4. OBJECTIVES OF THE DOCTORAL THESIS

4.1 Definition of solved problem

The operational loading of the rail´s material is very complex, so the material response consists of a different ratio of the mentioned wear processes. To distinguish the decisive degradation mechanisms in real operational conditions, often as a source serious accidents, is very difficult and requires a deep materials analyses.

Current predominance of contact fatigue induced defects causes, that the main focus of the material research is an investigation of materials with improved dynamic yield stress, fracture toughness, i.e. with a stable tendency to ductile dynamic fracture mode. There are generally two ways to reach improved material resistance, and hence improved safety and service life of the standard pearlitic rail steels:

- Microalloying as a way to increase the dynamic durability of steel by microstructure refinement
- Surface heat treatment - currently widely used so-called “perlitization” towards to reduction of inter-lamellar space of pearlite, i.e. in principle the same effect as above-mentioned microalloying.

Different, very attractive way, is the application of materials with different structure base – bainitic steels. Finally, the introduced austenitic Hadfield steel presents superior dynamic resistance, but the necessary precondition is a dynamic hardening of surface layers.

One of the crucial problems of current research is an evaluation of real mechanical parameters of the surface layer, which is decisive for service behavior of all rail steels grades. Two main problems are connected with needed determination of real mechanical response of loaded surface layers of rail profiles:

a) The commonly used mechanical parameters according to the valid standards do not reflect the real resistance to complex loading in the railway system. Specialized tests, which enable the simulation of rolling contact process at exactly defined loading parameters, are necessary.

Very important is the ability to precise control of the contact pressure and tangential slip values.

b) It is impossible to evaluate the mechanical parameters of surface layers, because of small depth from the surface and the structural and mechanical heterogeneity. The indentation hardness test, including the elastic-plastic response measurement, presents the prospective way how to contribute to the solution of this problem.

4.2 Aim of research

The aim of the doctoral thesis is to find out the possibility for evaluation of the real state of surface layers of railway steel in different mechanisms and stage of degradation. From the point of subjected materials, the evaluation will focus on Hadfield steel compared to standard pearlitic steel of the R260 grade. The explosive treatment of Hadfield steel will be involved in experimental testing to evaluate its influence on resistance to typical degradation process in the hardened surface layers.

To distinguish the decisive degradation process, the structural and phase analyses will be performed. The structural and connected mechanical changes, typical for the rolling-contact process will be induced by simulation of operational effects using the special rolling stand with is available at Educational and research center in transport. Validation of simulated effect will be based on comparative analyses of operational degradation of the same type of steels.

The main point of research is to suggest the suitable way for evaluation of the induced mechanical heterogeneity of the surface layers. Comparative indentation test will be conducted using different indenters and the new methodology for direct determination of elastic limit will be tested.

5 ANALYSES OF OPERATIONAL DEGRADATION AFTER OPERATIONAL LOADING

According to the focus of research, Hadfield steel was analyzed after operational loading to find out the main degradation effects. Pearlitic steel, grade of R260 was considered as a comparative material. Results of degradation pearlitic structure presented the standard railway material response. Each structural effects will be discussed with a focus on the distinctive parameters of degradation process together with the main problems of metallurgy quality.

5.1 Specifics of pearlitic microstructure degradation

The surface microcracks initiation due to rolling contact fatigue is a typical effect of operational loading of the rail steels regardless the structural substance. The specific influence of pearlitic microstructure is created by the presence of structural free ferrite and also the plate-like morphology of cementite.

A cumulative plastic deformation creates the typical plastic flow; surface initiated microcracks are driven by this flow as it is documented in figure 22. The subsurface cracks initiation is typical only in case of inclusion presence, the kind of MnS is the most common type of inclusion in pearlitic rail steels (as is documented in chemical analyses in figure 23

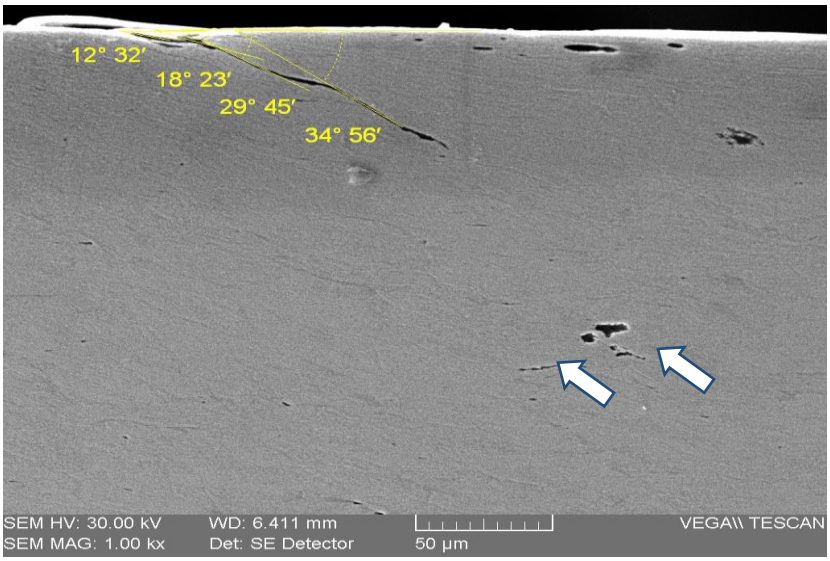

Figure 22 Rolling-contact effect on the pearlitic steel grade of R260 – state of Head check initiation

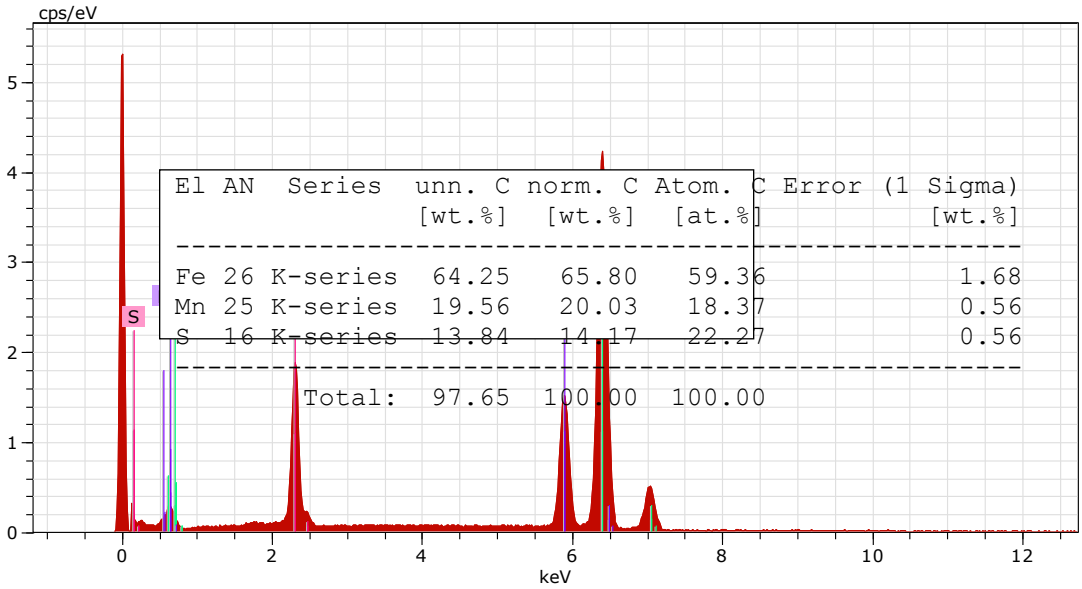

Figure 23 Identification of sulfides in connection with cracks initiation

The slope of cracks graduals up to the depth in which the cracks overcame the plastic flow; the branching of cracks secondary cracks can be observed in this stage of degradation – figure 24. Change of crack´s slope is a dangerous source of service cross-section fractures. Because of that, the ratio between the rate of crack propagation and depth of plastic flow is a distinctive parameter of operational safety.

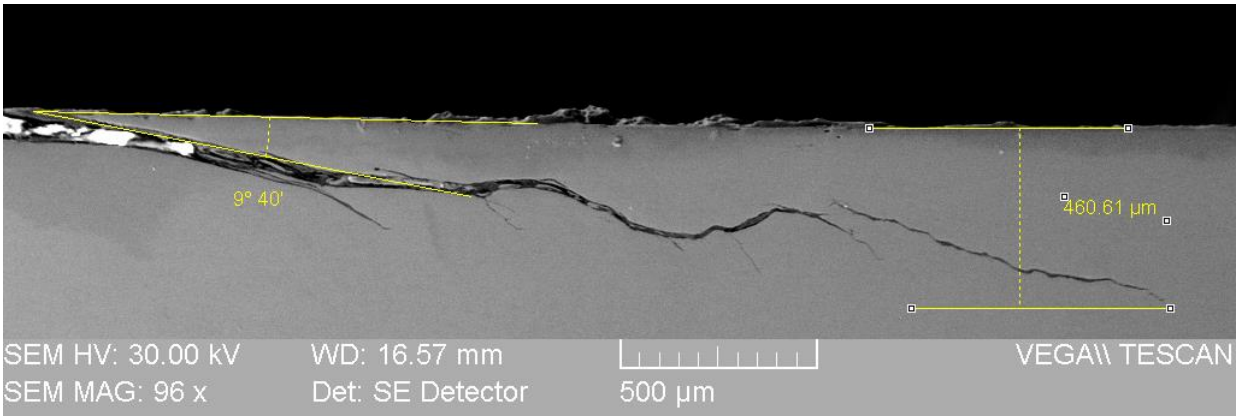

Figure 24 Stage of secondary branching of surface initiated cracks

From the point of ferrite effect, the proeutectoid ferrite is the source of predominant micro-cracks initiation and also the cracks propagation as seen figure 25. Because of that, the presence of this structural component is restricted mainly for heavy loaded parts of the railway

track. The continual presence of proeutectoid ferrite for steel grade of R260 can occur for example due to surface decarburization during high temper forming and it is accepted in a layer with a maximal width of 0.5mm. The acceptable intensity of decarburization is documented in figure 26.

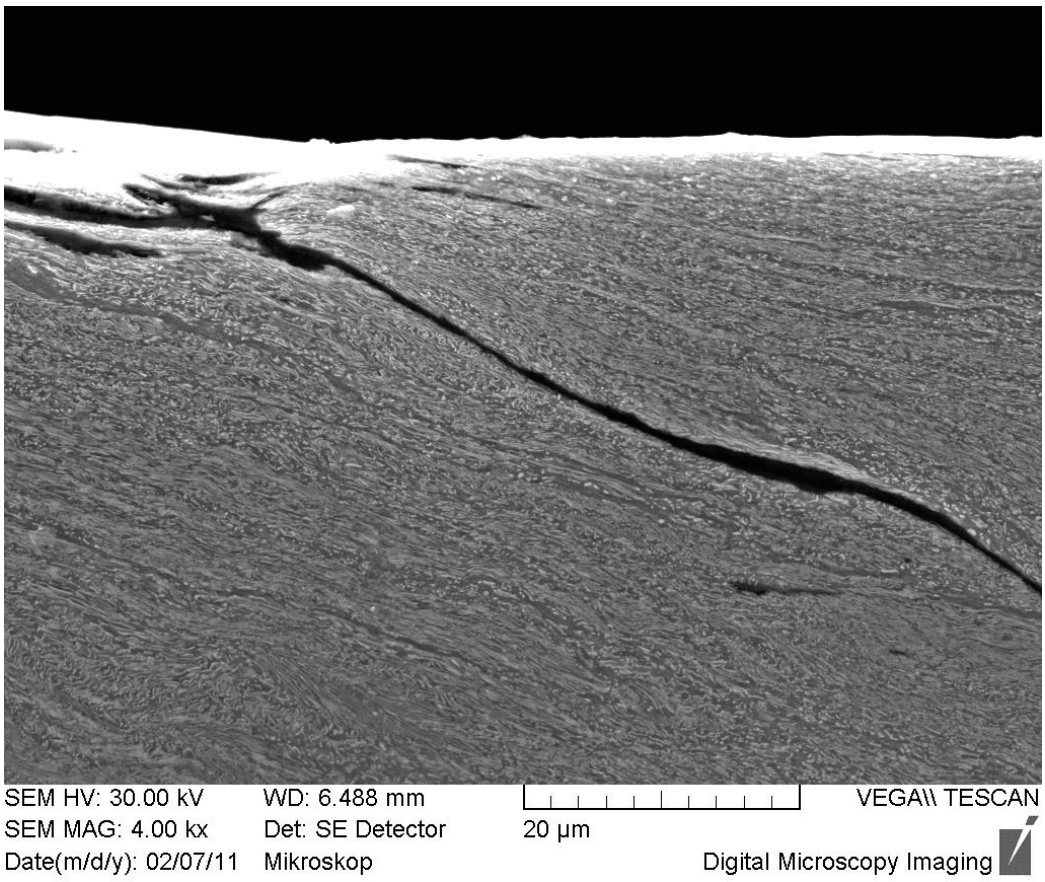

Figure 25 Detail of plastic flow created during rolling contact

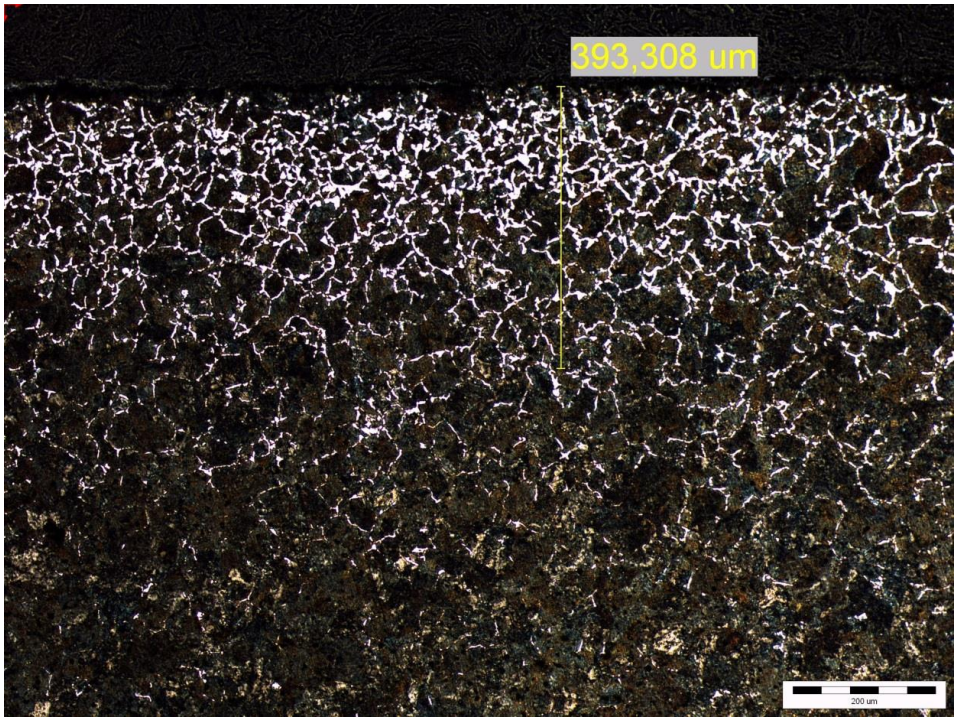

Figure 26 Decarburization of rail profile surface before loading

Important limited state of standard pearlitic rail steels is the creation of martensitic layers due to a local heating due to loss of adhesion. High sensitivity to this process is caused by high content of carbon – near to eutectoid concentration. The same is a reason of difficult weldability, i.e. the critical cooling rate is reached except especially used precautions.

The specific improving effect is discussed in some literature, as the desks of cementite may be oriented towards to loaded surface (thanks to the plastic flow), the wear rate and even the fatigue cracks initiation can be delayed. But this process is often connected with the white etching layers creation.

5.2 Specifics of Hadfield steel microstructre degradation

Samples for the analyses of actual degradation mechanisms were cut out from a railway switch in position, where the contact track was 40mm in width, i.e., in a position characterized by high dynamic operation loading. The chemical composition of the tested Hadfield steel was in full accordance with the standard EN 15689.

Because of the casting form and high content of alloying elements, mainly manganese, the Hadfield steel´s degradation effects differ from the pearlitic one significantly. Next parameters are the most important from the point of fatigue resistance:

(a) Grain size and morphology

The high content of manganese and fully austenitic microstructure is the source of the high sensitivity to the grain coarsening; typical Hadfield structure contains large grains- as seen figure 27. Grain size differs according to the local cooling rate, e.g. the real castings are very inhomogeneous in each position. The grain size heterogeneity is the source of heterogeneous deformation response, mainly under dynamic loading.

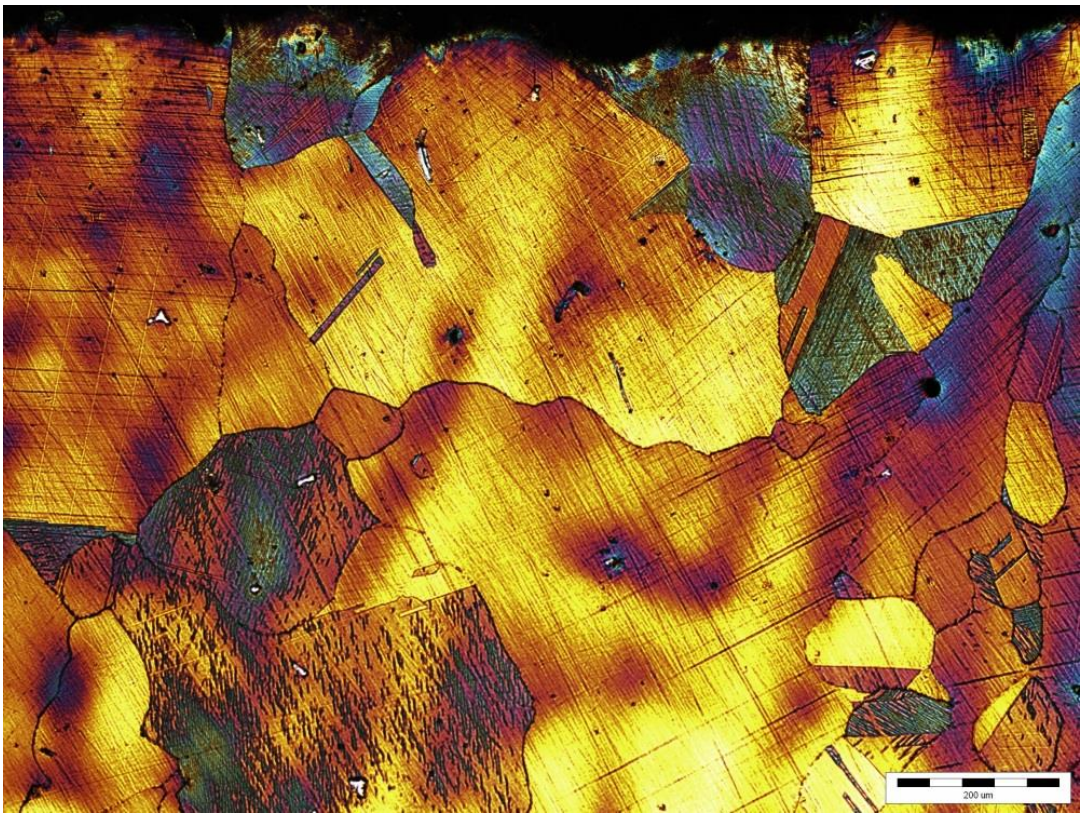

(b) Metallurgical defects

In the high manganese steel casting process, there are many types of casting defects, such as shrinkage cavity, micro cracks, and composition segregation, etc. these defects cause longitudinal cracks, vertical cracks and worst case failure and derailment. Because of this, service life of frogs and switches are limited. Hadfield is produced by casting method which results in impurities in structure. Hadfield steel earns its toughness by work hardening. Effect of hardening

shows itself as dislocations over substructures. This dislocation and the hardening effect are not uniform over the steel layers. , microscopic observations show that evolved substructures of the Hadfield steel subjected to deformation are mostly non-homogeneous. This is the reason of impurities in steel due to casting. In figure 28, non-uniform dislocations can be seen around ***micro-shrinkage***. This non-homogeneous deformation results initiating cracks.

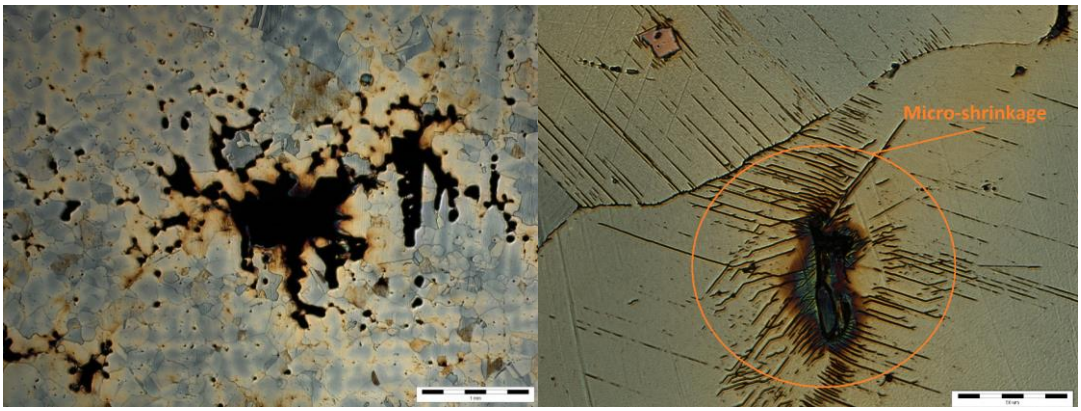

Figure 28 Macro vs. micro casting defects

(c) Intensive dislocation hardening

Hadfield steel has a non-uniform distribution of hardness in figure 29 (as a result of non-homogenous deformation) all over space which is influenced by grain orientation and microstructures (or impurities presence) which result near surface cracks as seen figure 30. This non-homogenous hardness can be determined by indentation methods and micro-tensile tests. In a further section, indentation methods and results will be explained.

Figure 29 Hadfield steel has a non-uniform distribution of hardness

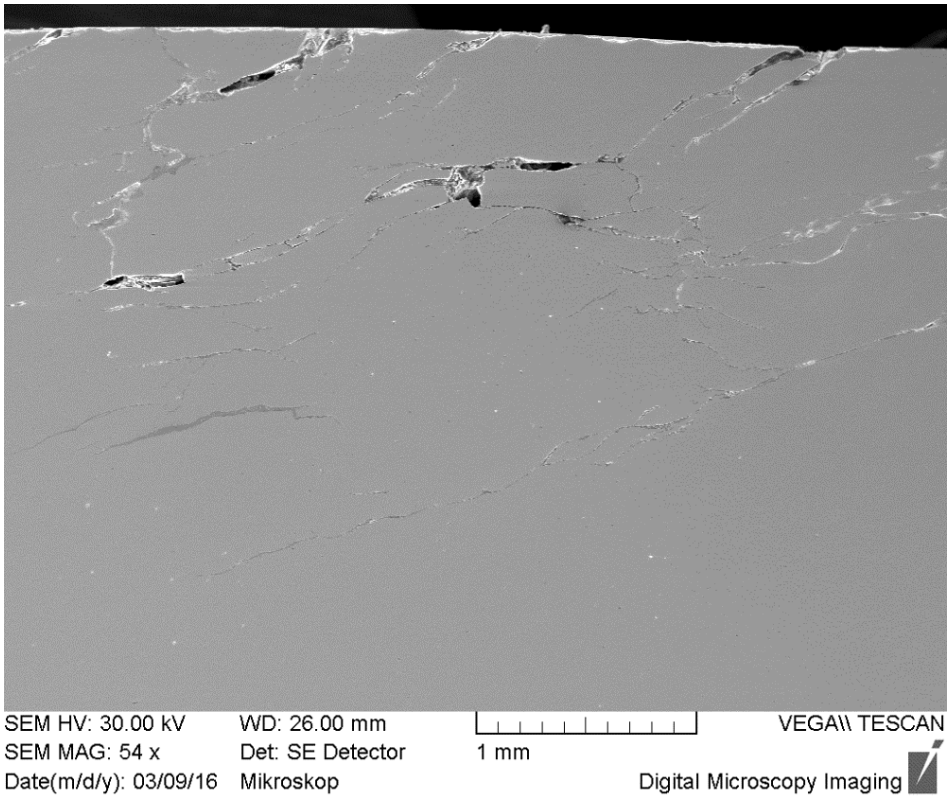

Figure 30 Surface fatigue cracks

(d) Intergranular carbide precipitation

Very specific for Hadfield steel is tendency to the carbide precipitation and even in some cases the phosphide eutectic creation which results in corrosion and cracks as seen figure 31

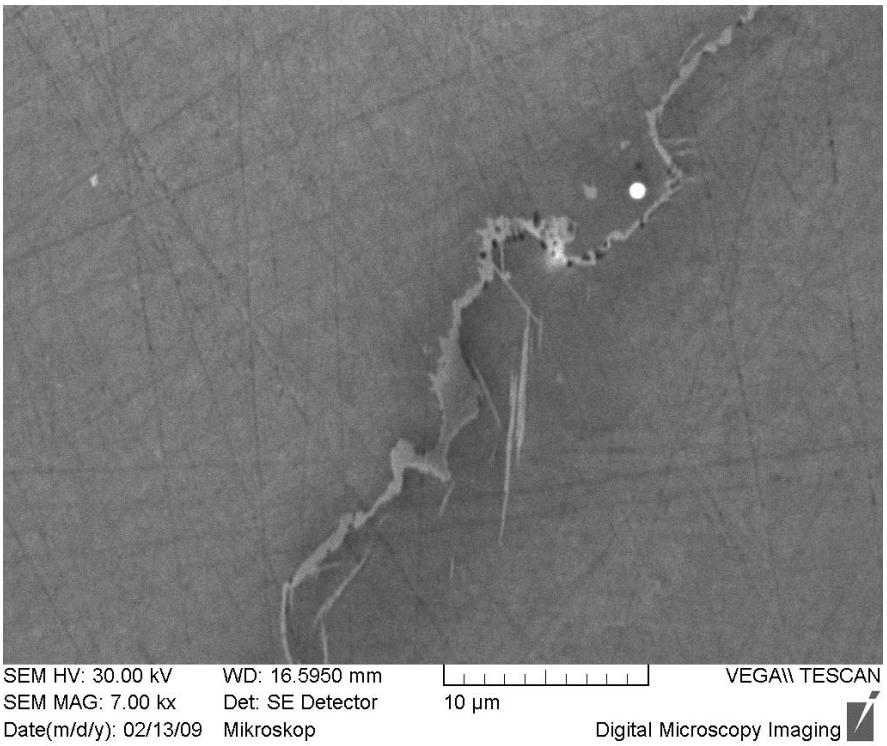

Figure 31 Intergranular carbide precipitation in Hadfield steel

6 ANALYSES OF OPERATIONAL DEGRADATION AFTER EXPERIMENTAL LOADING (ROLLING CONTACT TEST)

The comparative rolling contact fatigue (RCF) tests were performed:

a) using the standard pearlitic steel grade of R260
b) using the Hadfield steel

The dynamic response of the Hadfield steel was evaluated in two conditions - after the typical fabrication process vs. after the explosive hardening process. The influence of explosive hardening on degradation mechanisms was assessed within this experiment.

6.1 Methodology of the test

The degradation process was simulated by a specialized wheel-test rig which enables rolling contact loading at a defined ratio between contact pressure and longitudinal slip. The contact was induced between a wheel 920mm in diameter and a special sample holder - a disk 136mm in diameter. The principle of the test is displayed in figure 32.

Loading parameters:

- contact pressure P_{max}= 1140MPa
- relative longitudinal slip s = 1%
- revolutions: 400rpm (at the beginning of the experiment)

The tested samples can be pulled out from the holder (figure 33) during the test and can be subjected to complex material analyses in chosen stages of the fatigue test. The presented test was focused on the degradation mechanism in defined stages of the rolling contact loading, so the evaluation consisted of the following parameters:

- surface hardening (in HV10 hardness values),
- the depth of the plastic zone,
- character and depth of the surface damage (i.e., the slope and depth of the surface microcracks),
- and a wear rate, measured by the weight loss between defined steps of the loading.

Experimental loading was adjusted to the real operational ratio between the normal loading and longitudinal slip. Strengthening effect of the surface layer was monitored at chosen loading stages and verification of experimentally induced degradation process was based on structural analyses of the operational induced process. Instrumented indentation test was employed for evaluation of elastic-plastic capacity under the influence of hardening in compared states of Hadfield steel.

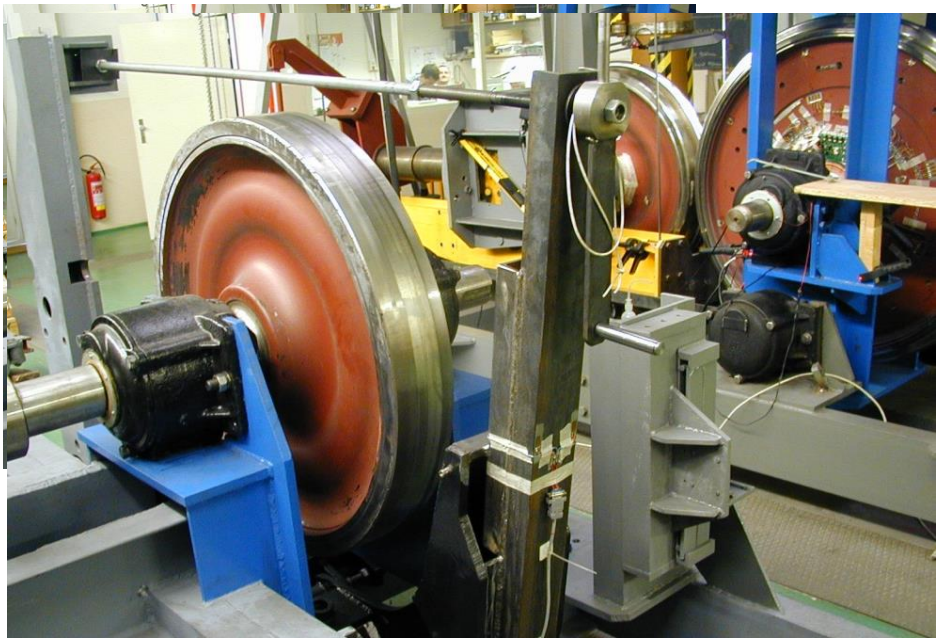

Figure 32 Rolling contact fatigue testing equipment

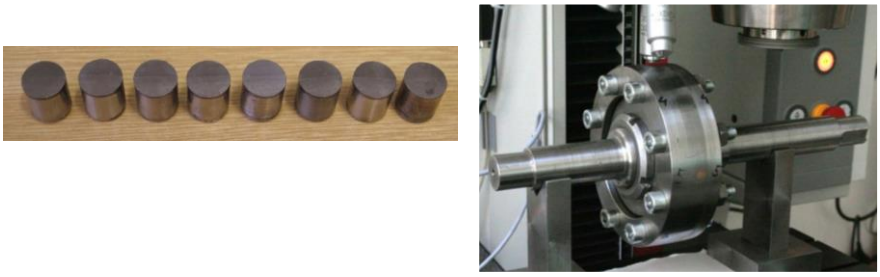

Figure 33 The holder for set of tested samples

6.2 Results and discussion

Deformation hardening of surface layers was evaluated per 100 thou. cycles; average values from 3 measurements of each of the 4 samples' surfaces are shown in figure 34-36

Pearlitic steel:

Pearlitic steel displayed hardening up to 500 km hardness was measured by dynamic equipment Equotip2. Intensive decarburization can be estimated as a source of lowered initial hardness. Continual wear of surface was typical during the whole loading time – see figure 34-35

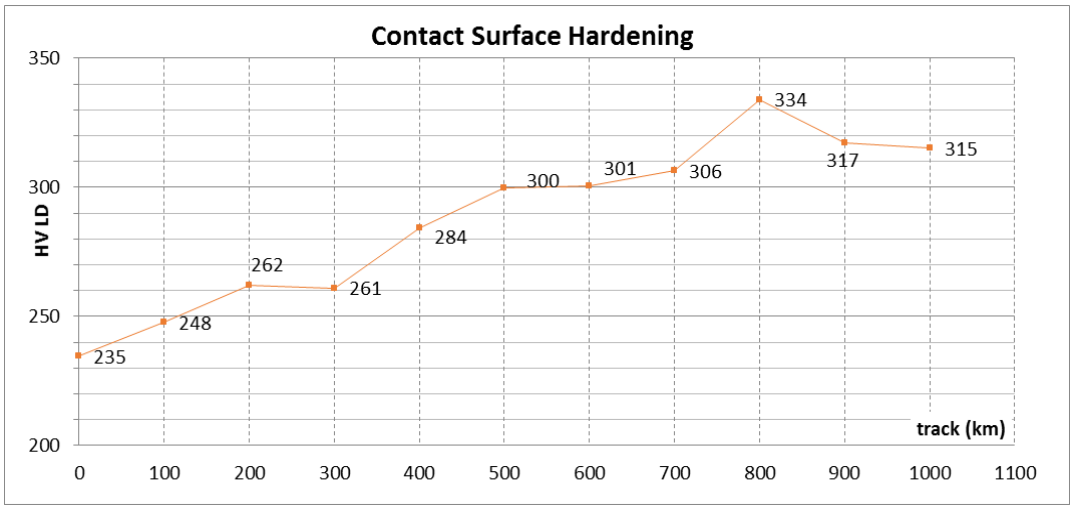

Figure 34 Hardening under rolling contact test

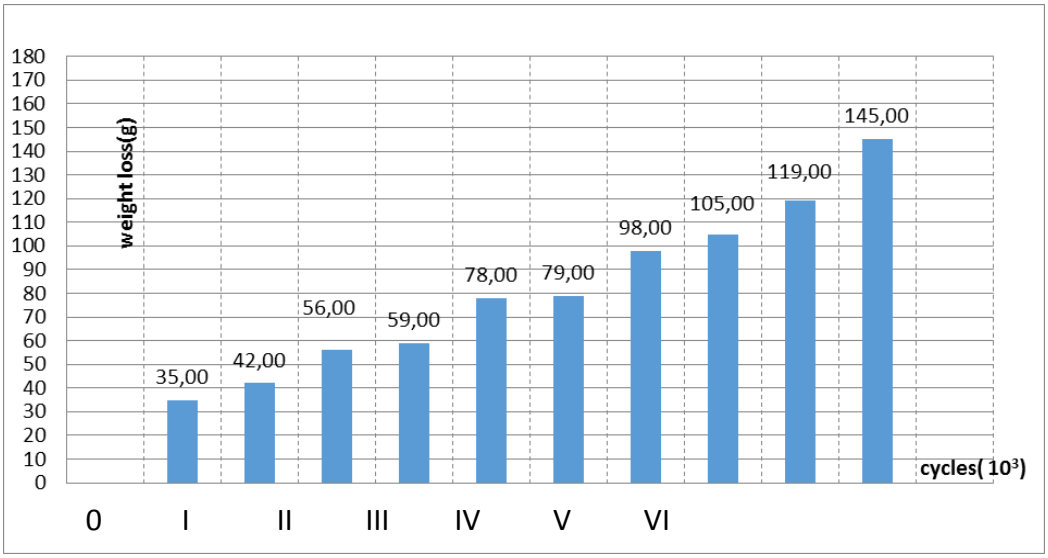

Figure 35 Weight lost under rolling contact test

Hadfield steel:

Intensive surface hardening of Hadfield steel was induced in the early stage of loading for both states of Hadfield steel. A sharp rise in hardness together with minimal wear appeared

during the first 200 thou. loading cycles. At about 300 thousand loading cycles the biggest weight losses were ascertained for both compared states of the Hadfield steel, and earlier onset of intensive wear for material without explosion hardening. The tip of the observed wear progress was slightly moved to the higher loading cycles, and the global wear range of the steel after explosive hardening was lower compared to the material without prior hardening. A similar gradient of hardening depending on the number of loading cycles was ascertained up to approximately 800 thou. cycles. Saturation of the hardening vs. wearing processes occurred during subsequent loading cycles.

The main difference compared to the pearlitic steel was saturation effect of Hadfield steel; the hardening over 500HV was connected with wear reduction.

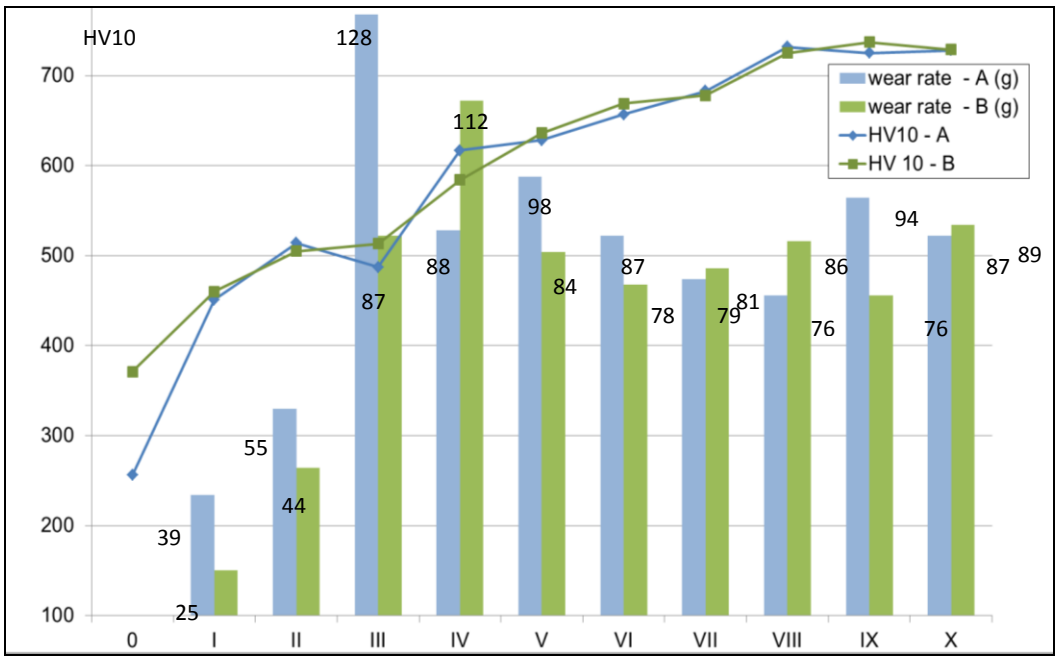

Figure36 - hardening process vs. wear rate induced by experimental contact loading, in HV10 values (A…samples without explosive hardening, B… samples after explosive hardening)

The structural analyses were performed in the final state of examination, i.e. after 1mil. loading cycles. Samples which is taken from disk polished, ground and etched for the preparation of metallography.

Pearlitic steel:

Intensive scaling was typically observed on the surface of pearlitic steel as seen figure 37.Important parameter from the point of operational safety is the depth of plastic deformation. As the plastic flow influences the orientation of surface initiated cracks, the secondary branching of cracks is restricted within this layer.

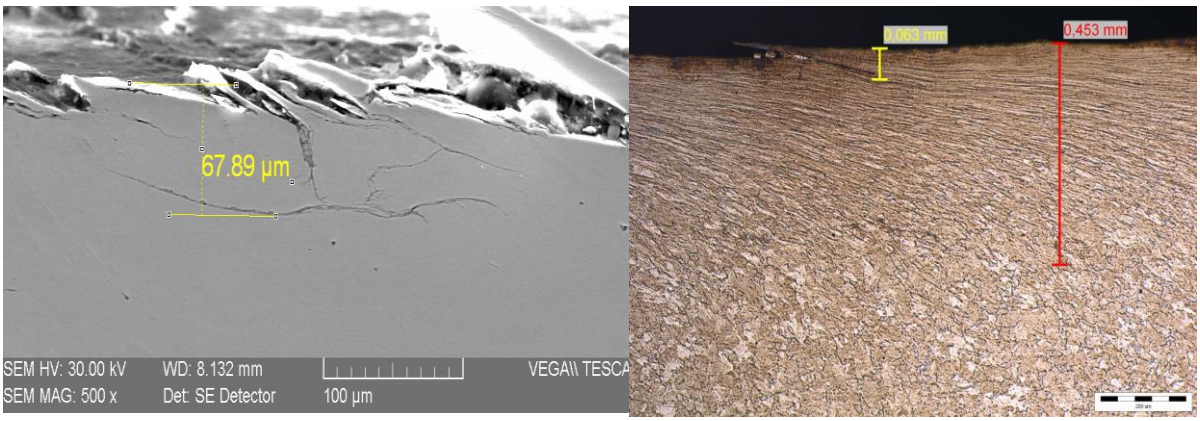

Figure 37 Pearlitic steel - depth of plastic deformation vs. depth of surface initiated cracks

Hadfield steel:

Intensive dislocation hardening up to a depth of 700 µm was observed by metallographic analysis in cross sections directed according to rolling contact in Fig.2. White etching layer (WEL) is a phenomenon that occurs on the surface of rail when it is in service due to the action of wheels. Its name arises from its resistance to etching by acids(figure 38) during metallographic preparation and its white featureless appearance under the optical microscope. Sample was etched to observe WEL can be seen figure 39

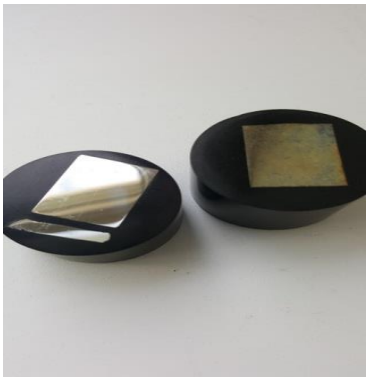

Figure 38 Etched sample (on right)

It is commonly found in patches, approximately 20–100 μm deep, on the surface of rail after it has been in service for several months [26]

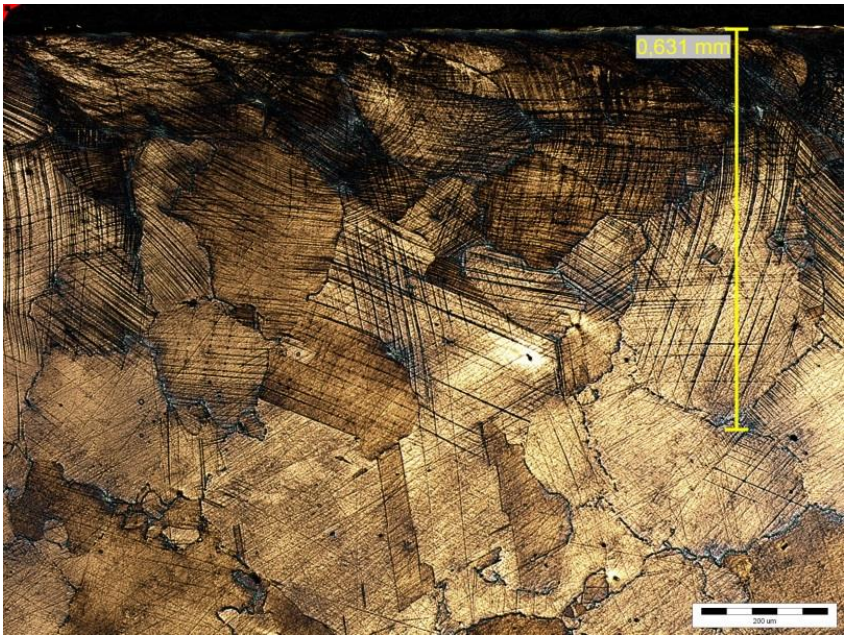

Figure 39 Hadfield steel - depth of the whole dislocation hardening

Contrast phase was created by simulated contact fatigue up to a depth of 30μm, typical was a different level of plastic deformation inside these layers. The voids and microcracks are created directly in this layer approximately perpendicularly to the contact surface, apparently as a consequence of fragility of these microvolumes.

The different degradation process was connected with ductile shear caused by the progressive shear deformation. Surface fatigue cracks are initiated and propagated by a low cycle fatigue mechanism, driven by cyclic plastic strain. While the microcracks in the "WELL" was subjected to the intensity of inhomogeneous deformation(figure 40-41), the RCF cracks followed the plastic flow. In the operational conditions, the surface cracks due to RCF, well known as a "Head check", are perpendicular to the running direction of the wheel. Results of the hardening gradient measurement as a degradation process evaluation is discussed in chapter no.7.1.

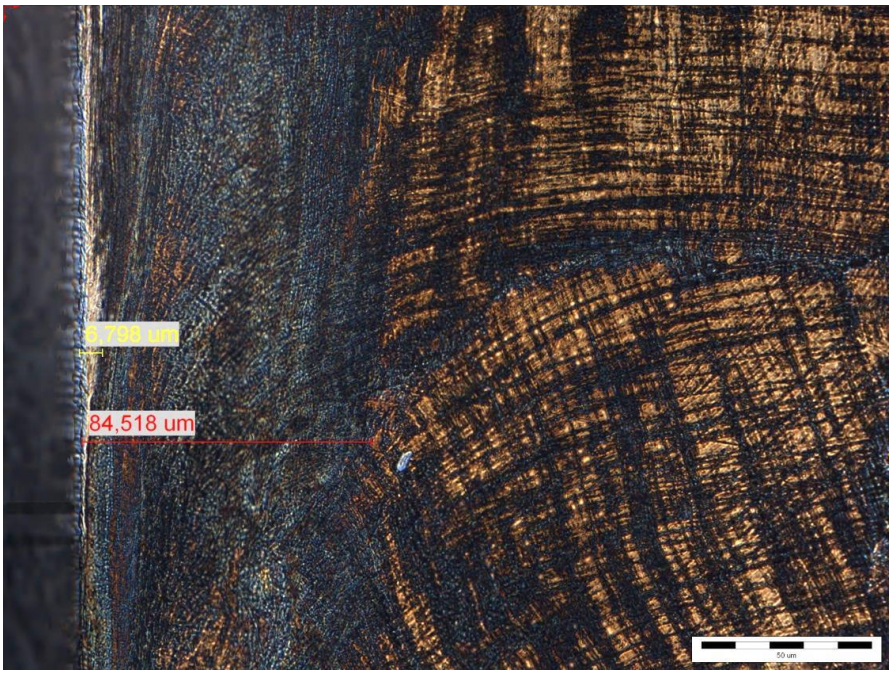

Figure 40 Depth of localizing dislocation hardening vs. creation WEL-like layers

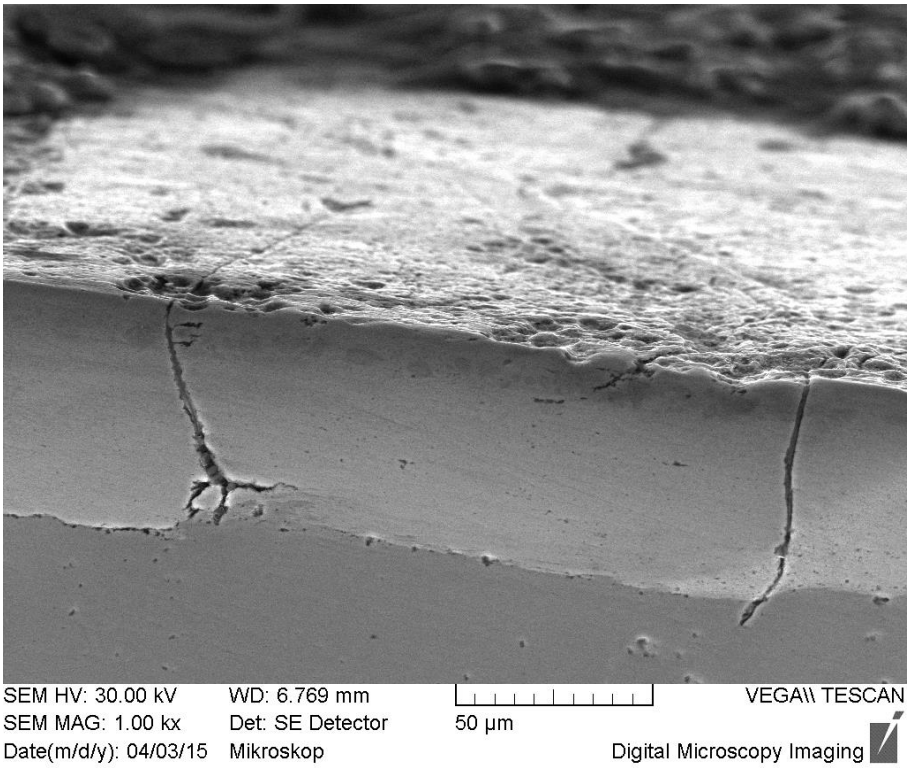

Figure 41 Creation of "WEL" like surface layer

7 THE INDENTATION METHOD

Indentation test is necessary for the monitoring of the force and indentation depth relation and hardness value of the material. In other words, hardness measurement displays mechanical behavior of materials. In this thesis, we will introduce 3 types of indtation method such as Vickers, cylindrical, spherical . All indenters have advantages and disadvantages according to the area of usage . Indentation techniques have been also used to investigate time and temperature dependent properties of metals such as creep and load relaxation, residual stress field, fracture toughness [33-36]. Recently, low-load indentation techniques such as nanoindentation have been developed for testing metallic and ceramic thin films or coatings [37].

The principle of the test procedure and energy evaluation was obtained according to **ISO 14577-1:2002(E).**

Elastic-plastic work against a force, hardness value and mechanical behavior of a material can be determined from indentation depth- force graphs.Test machine shall have the capability to fulfil requirements of ISO 14577-2. Zwıck test machine which can able to apply up to 2500 N has been used for all of the experimental procedure.

For accurate experimental procedure according ISO 14577-2:

- Test sample should be clean, free of lubricant, smooth surface and polished
- The temperature of test should be controlled. Sample should reach ambient temperature before testing and testing machine should provide stable temperature for testing sample
- Test force shall be applied without shock and vibration which can significantly affect results
- It is important that the test results are not affected by the presence of an interface. Previous plastic deformation due to indentation test can effects new result (work hardening) because of that new test should be applied far from previous measurement point.

Parameters determined from force indentation data set

It is possible of determination of hardness and several parameters during recording loading and unloading cycle by instrumented indentation. Unlike simple hardness machines, Instrumented indentation give us a set of data including force, depth and time with high accuracy. It is possible to evaluate elastic-plastic behavior, martens hardness, and material characteristic. Using a force- or indentation depth controlled test cycle delivers information as to the creep or the relaxation of materials. Recently, there has been growing interest in by depth and time controlled indentation will let us determine time-dependent deformation behavior including polymers [38–45], foods [46] and even biological tissues [47–52].

Martens hardness HM:

Martens hardness is determined by indentation depth curve during increasing of test force it is defined as the test force F divided by As(h) the surface area of the indenter. It can be calculated just by pyramidal types indenters (such as Vickers)

Martens hardness determined from force- indentation depth curve HMs:

The method is used for the determination of the Martens hardness by using the slope of force indentation depth curve. It has the advantage of avoiding zero-point determination for homogeneous materials.

Determination of elastic-plastic work:

The force controlled test procedure can be seen figure x, Firstly, machine apply force until to reach a maximum point, until this point it is possible to determine total work energy of material and martens hardness.

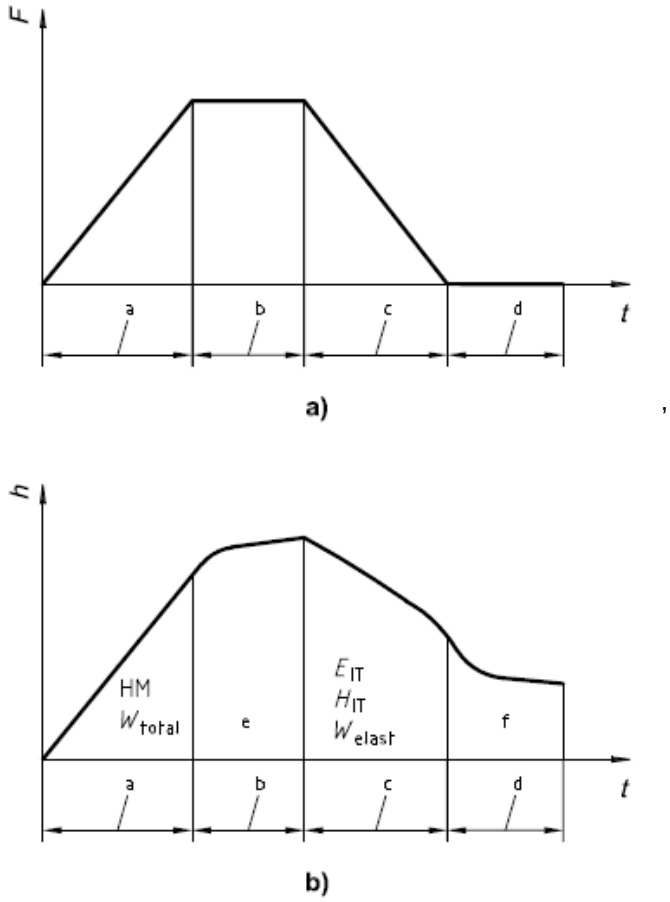

a Application of test force
b Maximum test force
c Removal of test force
d Test force = 0 N
e Indentation creep
f Recovery at zero test force

Figure 42 Determination of elastic-plastic work

After reaching maximum force point, the machine removes the force and relaxation curve start (c removal of test force) at this point elastic work of material can be defined. In another word, the mechanical work *W*total indicated during the indentation procedure is only partly consumed as plastic deformation work *W*plast. During the removal of the test force, the remaining part is set free as work of the elastic reverse deformation *W*elast. Which can be seen figure 42[ISO 14577-2]

The test procedure can be force or displacement controlled and the test force F, and indentation depth h was recorded during the experiment. The typical force indentation depth graph can be seen figure 43. This graph includes just indentation curve to obtain elastic behavior of material and relaxation curve. This stage Vickers indenter was used and observed indentation depth change corresponding to linear force increase.

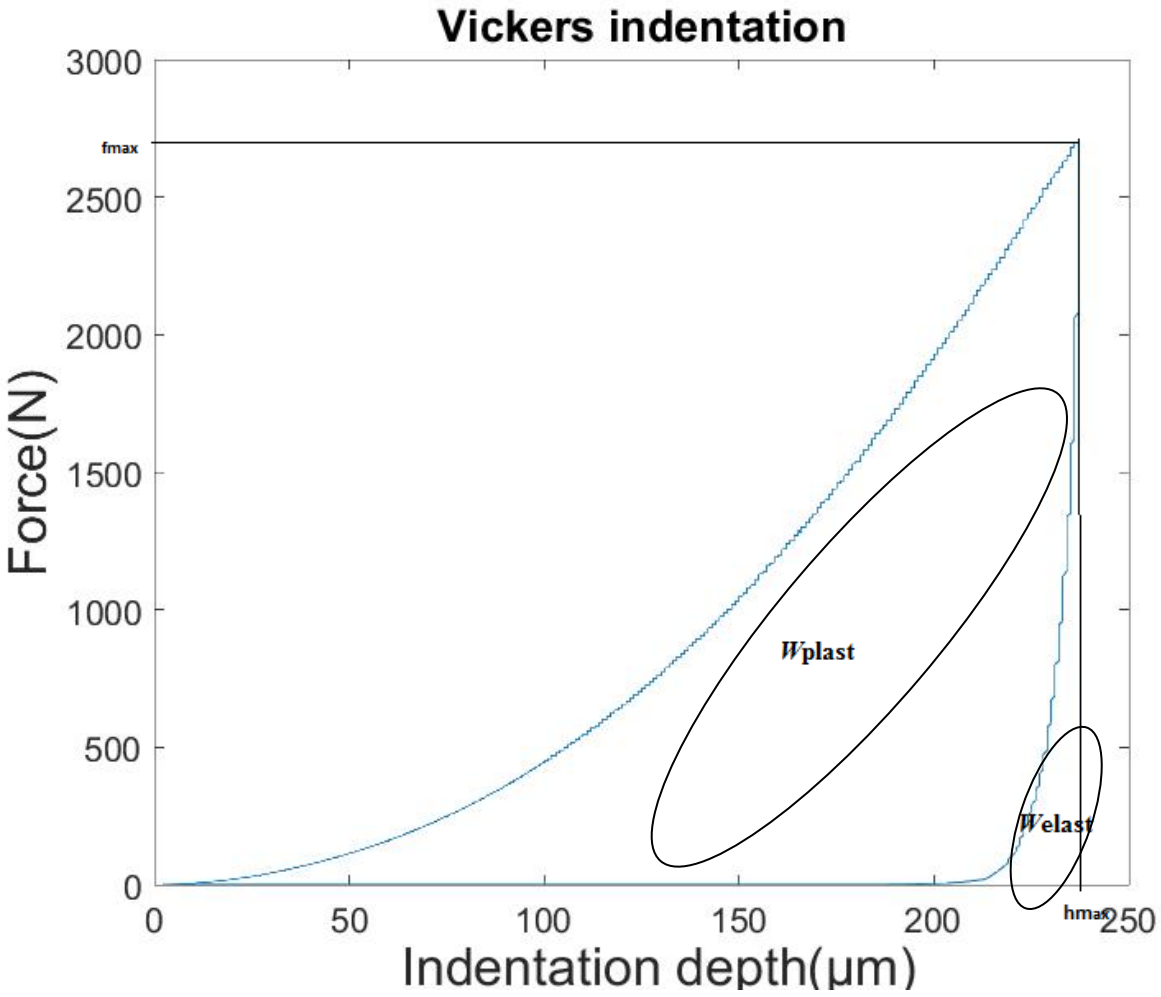

Figure 43 Physical behavior of Hadfield steel under Vickers indentation

7.1 Evaluation of Elastic-Plastic response of Hadfield by Vickers indentation testing

The Vickers hardness test was developed in 1921 by Robert L. Smith and George E. Sandland at Vickers Ltd as an alternative to the Brinell method to measure the hardness of materials [29].

Several measurements have been applied according to ISO 14577-2 standard, in this thesis, we used standard Vickers indentation for samples; before rolling contact (with, without explosion hardening), after rolling contact (with, without explosion hardening) All results are recorded in the tables below.

We obtained data:

HV10=Hardeness measured by optical microscope

HM=Martens hardness

HM S= Martens hardness, determined from the slope of the increasing force/indentation depth curve

***W*elast=** Elastic reverse deformation work of indentation Nmm

***W*plastic=** reverse deformation work of indentation Nmm

***W*total =**Total mechanical work of indentation Nmm

η_{IT}= Relation *W*elast /*W*total %

hmax = Maximum indentation depth at *F*max

Δ (1 vs 2) =difference between average values table 1 and table 2

Δ (3 vs 4) =difference between average values table 3 and table 4

Table 1 Before rolling contact without explosion hardening

Number of measurement	HV 10	HM	HM_S	*W*elast	*W*plastic	*W*total	η_{IT}	hmax
	N/mm²	N/mm²	N/mm²	Nmm	Nmm	Nmm	%	µm
1	253	1913	1849	0.223	1.266	1.489	14.99	44.05
2	251	1665	1635	0.237	1.309	1.545	15.32	47.21
3	250	1964	1875	0.222	1.256	1.478	15.03	43.48
4	265	2047	1795	0.234	1.26	1.494	15.68	42.58
5	267	1921	1839	0.268	1.244	1.512	17.75	43.99
6	253	1796	1836	0.229	1.264	1.493	15.33	45.45
7	264	1912	1778	0.295	1.249	1.544	19.13	44.11
8	247	1808	1607	0.328	1.277	1.605	20.44	45.37
9	256	1927	1724	0.244	1.264	1.508	16.15	43.9
10	252	1856	1826	0.279	1.252	1.531	18.22	44.72
Average	**256**	**1881**	**1776**	**0.256**	**1.26**	**1.52**	**16.8**	**44.49**
σ	**7**	**105.6**	**93.5**	**0.036**	**0,018**	**0.038**	**1.94**	**1.28**

After obtaining all parameters, Explosion hardening was applied the same type of sample in table 1 to observe the changes. All result can be seen in table 2

Table 2 Before rolling contact with explosion hardening

Number of measurement	HV 10	HM	HM_S	*W*elast	*W*plastic	*W*total	η_{IT}	hmax
	N/mm²	N/mm²	N/mm²	Nmm	Nmm	Nmm	%	µm
1	368	2724	2719	0.213	1.015	1.228	17.331	36.92
2	365	2853	3060	0.203	0.973	1.177	17.285	36.06
3	364	2829	2839	0.211	0.988	1.198	17.578	36.24
4	371	2806	2971	0.197	0.99	1.187	16.619	36.38
5	369	2731	2709	0.21	1.029	1.239	16.958	36.86
6	373	2951	2851	0.214	0.975	1.189	18.011	35.46
7	386	2946	2796	0.217	0.999	1.216	17.815	35.51
8	362	2632	2586	0.222	1.022	1.244	17.843	37.55
9	379	2743	2873	0.222	0.97	1.192	18.602	36.78
Average	**370**	**2801**	**2822**	**0.212**	**0.995**	**1.207**	**17.56**	**36.41**
σ	**7.67**	**105.94**	**142.8**	**0.008**	**0.022**	**0.024**	**0.59**	**0.68**
Δ (1 vs 2)	**-114**	**-920**	**-1046**	**0.044**	**0.265**	**0.313**	**-0.76**	**8.08**

Same samples were introduced rolling contact test machine to observe loading effect. Result of both with and without explosion hardened sample can be seen table 3, table 4

Table 3 After rolling contact without explosion hardening

Number of measurement	HV 10	HM	HM_S	*W*elast	*W*plastic	*W*total	η_{IT}	hmax
	N/mm²	N/mm²	N/mm²	Nmm	Nmm	Nmm	%	µm
1	738	3972	3711	0.387	0.661	1.048	36.966	30.58
2	734	5087	4976	0.323	0.614	0.937	34.444	27.05
3	733	4917	4732	0.348	0.589	0.937	37.163	27.53
4	722	4596	4447	0.351	0.616	0.967	36.264	28.46
5	726	3726	3485	0.385	0.705	1.09	35.354	31.6
6	732	4300	4238	0.387	0.601	0.988	39.138	29.42
7	729	4958	4583	0.321	0.626	0.948	33.906	27.4
8	715	3591	3894	0.395	0.645	1.04	37.998	32.15
9	747	3787	3279	0.41	0.692	1.102	37.188	31.3
10	744	3745	3369	0.423	0.678	1.101	38.408	31.51
Average	**732**	**4268**	**4071**	**0,373**	**0.643**	**1.016**	**36,83**	**29.7**
σ	**9.1869**	**579.39**	**606.60**	**0.0353**	**0.0379**	**0.0648**	**1.695**	**1.9681**

Table 4 After rolling contact with explosion hardening

Number of measurement	HV 10	HM	HM_S	*W*elast	*W*plastic	*W*total	η_{IT}	hmax
	N/mm²	N/mm²	N/mm²	Nmm	Nmm	Nmm	%	µm
1	737	2160	540	0.301	1.327	1.628	18.517	41.46
2	717	4769	4822	0.292	0.65	0.942	31.02	27.92
3	719	4157	4998	0.31	0.625	0.935	33.129	29.9
4	728	4172	4553	0.314	0.647	0.962	32.685	29.84
5	717	4245	4172	0.326	0.682	1.008	32.387	29.61
6	710	3950	4558	0.345	0.645	0.99	34.858	30.69
7	732	4225	5030	0.337	0.61	0.947	35.583	29.65
8	733	3552	3069	0.455	0.717	1.172	38.818	32.4
9	723	1491	5215	0.345	0.67	1.014	33.966	49.9
10	734	3090	2781	0.503	0.726	1.229	40.92	34.67
Average	**725**	**3581**	**3974**	**0,353**	**0.73**	**1.083**	**33,18**	**33.6**
σ	**9.06**	**1039**	**1459**	**0.0698**	**0.2130**	**0.2161**	**5.9763**	**6.9132**
Δ (3 vs.4)	**7**	**687**	**97**	**0.02**	**-0.087**	**-0.067**	**3.65**	**-3.9**

The evaluation of measured parameters was performed separately using the hardness measurement (figure 44) and energy consumption (figure 45).

Together with the study of explosive vs. rolling contact loading influence, we can discuss the predictive value of each parameter. They were assessed by the differences of average values vs. deviations of each set of measurement. Differences of the order were considered as a substantial.

Explosive hardening influence (before the rolling contact) was registered by all of the used hardness measurement methodologies, i.e. using the optic evaluation and also using the indention depth evaluation. Plastic energy contribution represented the main portion of the energy consumption decrease. Elastic part of energy consumption was not affected significantly, so the "η_{IT}" parameter is not very effective in this case.

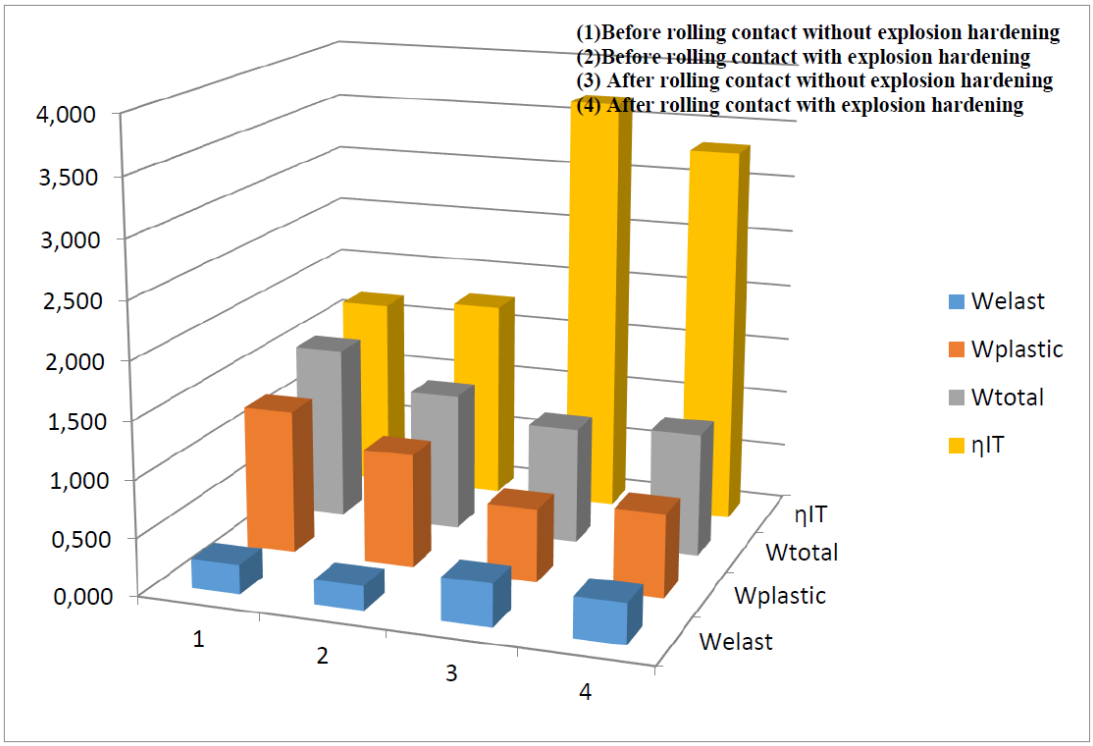

Figure 44 Comparsion of elastic-plastic work

Contrary to that, a rolling-contact loading influence was registered by the both type of parameters – hardness and also the energy consumption. Hardness was increased up to the level over 700HV for the both states of Hadfield steel – with and also without explosive hardening. The dominant influence of the contact loading was measured by the all of the used hardness evaluation methods.

From the point of hardening mechanisms it is interesting, that the rolling-contact loading decreased the plastic response together with the elastic energy increment. So the "η_{IT}" parameter has become effective for the contact fatigue process. Mentioned effect was measured for the both states of Hadfield steel – with and without explosion hardening (based on the comparison of the table(1) vs. (3) and also table (2) vs. (4)).

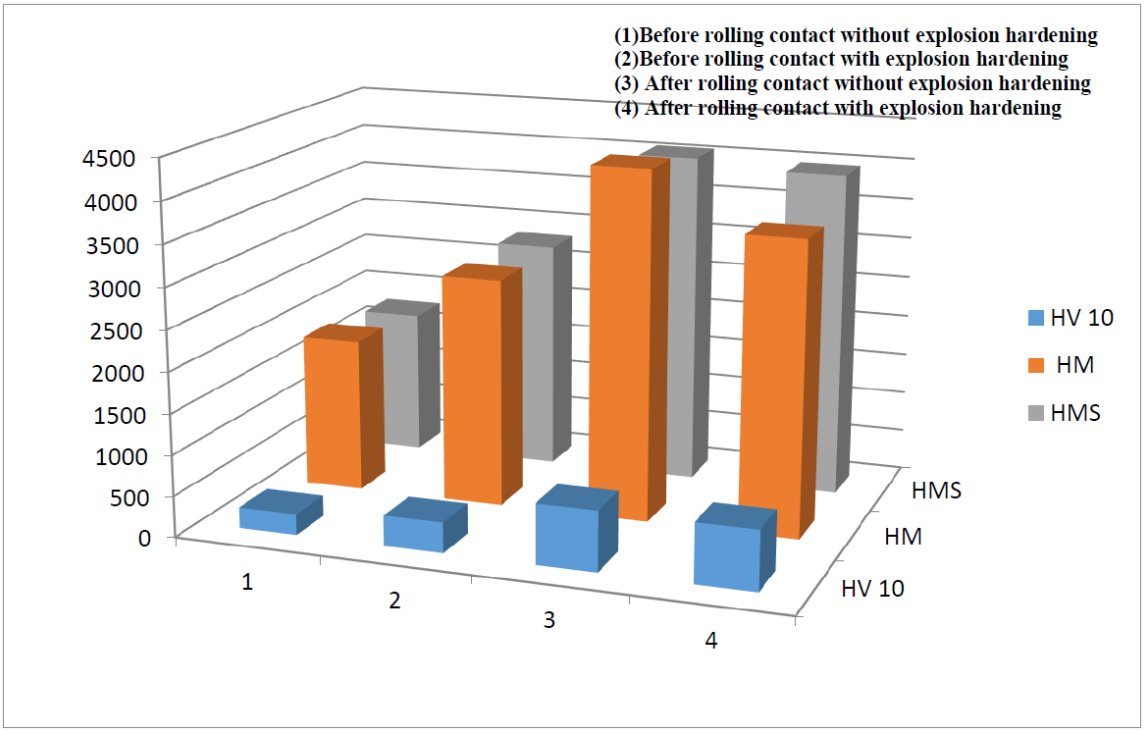

Figure 45 Comparsion of hardness values

The predominant effect of the rolling contact compared to explosive hardening was found out. Explosive treatment has led to approximately 45% increment of hardness. Regardless the primary state of hardening, the final stage of contact fatigue influence has reached almost the same level of the hardness and so the stage of plasticity depletion. It means the more intensive hardening (186% increasing) was reached in case without primary explosive treatment contrary to the hardening only 96% in case after explosive treatment.

Elastic energy ratio (registered by "η_{IT}" parameter) has confirmed the measured influence of explosive hardening; so the rolling-contact effect in the narrow surface layer was not affected by the explosive treatment significantly.

Indentation tests by using a Vickers indenter were performed for evaluation of the rolling contact effect in both stages of Hadfield steel – with vs. without explosive hardening (Tab.1, 2, 3, 4). The ratio of elastic and plastic deformation ($\eta_{IT} = (W_{elast} / W_{total}).100[\%]$) reflects the differing residual plastic capacity of the surface layer during rolling contact loading. The depth of the contact – fatigue strengthening needed to be determined for reliable measurements of the surface

layer state. The gradient of experimentally induced surface changes was evaluated by hardness measurement directed perpendicularly to the loaded surface .

The degradation process in rail-wheel contact was simulated for Hadfield steel in two initial states – with vs. without explosive hardening. Based on the performed structural analyses and indentation test we can conclude that the used experimental process is able to simulate the actual degradation mechanism up to achieving a specific limited state of the surface layers of Hadfield steel. The used methodology enables evaluation of the degradation process in particular stages of loading.

In the second stage, Vickers indenter according to the standard ISO 14577-1 was used for depth of hardening evaluation as seen figure 46. The depth of contact–fatigue strengthening was necessary to determine for reliable measurements of surface layer state. The gradient of experimentally induced surface changes was measured by hardness changes directed perpendicularly from loading surface towards to the axis of samples. Hardness test was applied by the 200-micrometer interval. Figure 46 presents the differences in intensity and depth of strengthening for compared stages of tested steel – with vs. without explosive hardening. Intensive surface hardening was induced in the early stage of loading for both states of Hadfield steel.

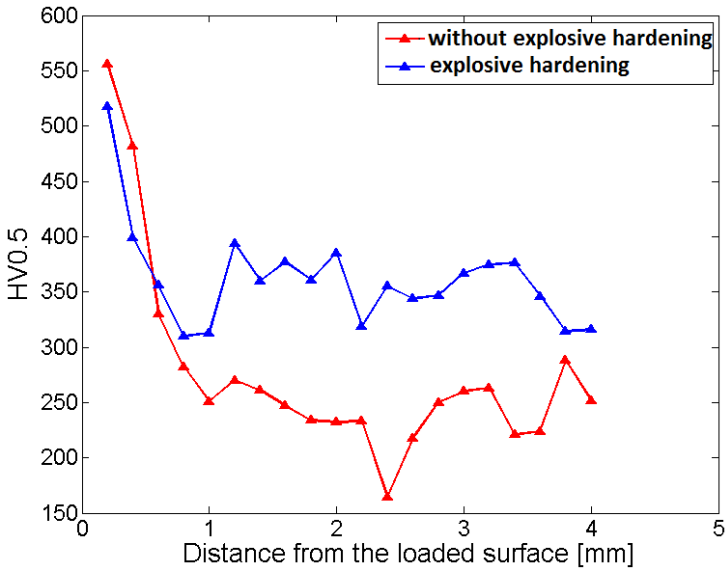

Figure 46 Hardness gradient of the compared stages of Hadfield steel

7.2 Evaluation of Elastic-Plastic response of Hadfield by cylindrical indentation testing

Comparative yield stress CYS [N/mm^2] was determined by using 1.2 mm cylindrical indenter which was applied to obtain indentation depth corresponding to linear force. HV (N/mm2) was found bellow. As represented in Fig15, this curve tends to be a tangential curve. Indentation depth is increasingly increasing characteristic corresponding to force until yield point;

- Before rolling contact after explosive hardening: 1699 N/mm2,
- Before rolling contact without explosive hardening: 878 N/mm2,
- After rolling contact after explosive hardening : 2290 N/mm2,
- After rolling contact without explosive hardening: 1696 N/mm2,

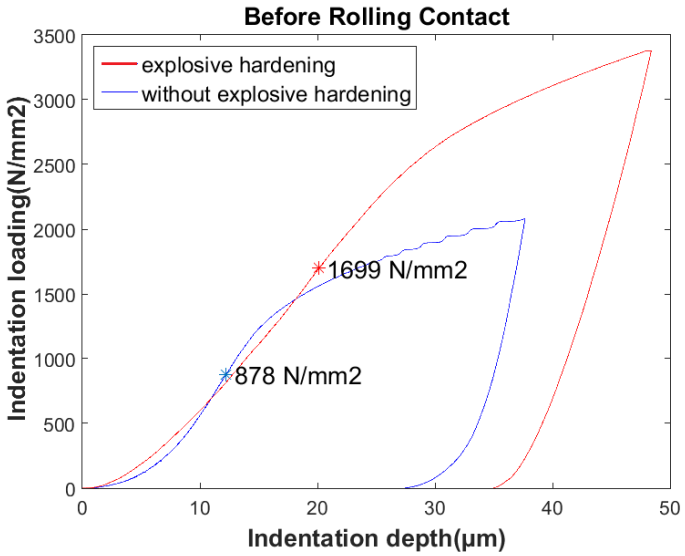

Figure 47 Finding Comparative yield stress CYS [N/mm^2] by using cylindrical indenter (Before rolling contact)

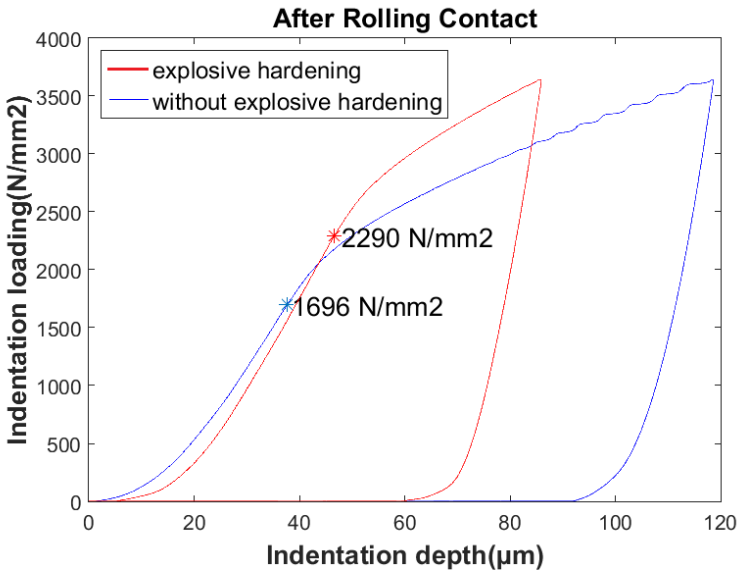

Figure 48 Finding Comparative yield stress CYS [N/mm^2] by using cylindrical indenter (After rolling contact)

The evaluated points give us transition zone of elastic to plastic deformation. Tests were performed for two samples which are explosive hardenened and without explosive hardening. According to hypothesis [29] about behavior of the material during extrusion of a cylindrical indenter, we used the constant 2.57 as a ratio of compressive stress applied by indenter to shear yield stress

Table 5 Parameters of elastic-plastic response at analyzed states of Hadfield steel

State of steel	HV 10	HM [N/mm^2]	h_{max} [μm]	W_{elast} [N.m]	W_{plast} [N.m]	W_{total} [N.m]	η_{IT} [%]	CYS [N/mm^2]
A	256±7	1881	44.49	0.256	1.264	1.52	16.80±1.94	341
B	371±7	2542	46.38	0.212	0.998	1.21	17.54±0.57	661
C	732±10	4268	29.7	0.373	0.643	1.016	36.68±1.70	659
D	725±9	3581	33.6	0.353	0.73	1.083	33.188±5.98	891
X	708±14	4201	28.73	0.316	0.688	1.004	31.459±6.24	

A - without explosive hardening /without contact loading, B - explosive hardened/without contact loading, C - without explosive hardening/after contact loading, D - after explosive hardening /after contact loading, X - representative surface state after operational exploitation)

All parameters in table 5 are taken from average Vickers measurement data(Table 1,2,3,4) .Standard tensile tests has shown the elastic limit σ_y = 368MPa for the primary state of Hadfield steel, i.e. for as-cast condition without explosive hardening and before operational loading. A particular difference between results obtained by indentation (figure 47-48) may be caused by intensive dislocation hardening during the fabrication of samples for tensile test and intensive local heterogeneity in grain size, which is typical for Hadfield steel. Despite that, the ratio between comparative yield stresses in evaluated states of analyzed steel (samples A– X in the Tab.5) reflects the influence of explosive hardening on the sensitivity of Hadfield steel to the depletion of plasticity due to rolling contact.

The evaluation of the elastic limit by indentation test using the cylindrical indenter has some limitations. One of that is state of the surface; damaged contact area doesn´t allow the precise measurement. Very high intensity and low depth of hardening are the restrictions for reliable measurement because of the influence of much softer zone below the surface. The usage of spherical indenter can be a solution in this situation.

7.3 Evaluation of Elastic-Plastic response of Hadfield by spherical indentation testing

Spherical indentation method is one of the most convenient methods of identification of elastic- plastic response of the material .This method proposed by Huber and Tsakmakis [60]. Solution of the spherical indentation problem also was proposed in papers by Hill et al. [53],and Biwa and Storakers [54].Besides that, Attempts to make use of spherical indentation testing to identify the elastic-plastic behavior of material has been considered in numerous papers. [55-57],

7.3.1 Capabilities of Spherical Indenter

We introduced the cylindrical indentation to determine comparative yield stress CYS [N/mm^2] in the previous chapter. Cylindrical indenter with a diameter of 1.2 mm was applied to obtain indentation depth corresponding to linear force to examine the effect of explosive hardening [31].

This section, the spherical indentation method was introduced to obtain more accurate results for the rough(uneven) surface. Force-Indentation depth graphs will be examined by the specific

method, moreover, real rail sample, with or without explosive hardening samples were compared by means of the new method.

Because of intensive operational damage of surface layers together with a typical material heterogeneity of Hadfield steel, the standard evaluation by cylindrical indentation is limited. Spherical indenters give better results for rough surfaces and also results are less affected by micro-cracks, grain boundaries, and typical micro-casting defects. It means that it is possible to measure hardness near crack zone with a spherical indenter. Besides that, spherical indentation methods let us a direct surface measurement without cutting off samples.

Larger diameter indenters effect larger area and give more accurate results. However, choosing large diameter is limited because of force capacity of hardness machine. We commonly used 5mm diameter spherical indenter to determination of mechanical behavior.

Unlike pointed indenters, elastic-plastic, and fully developed plasticity regime of material can be determined by spherical method because spheres possess the unique ability to transition through perfectly elastic to fully developed plasticity zone. Cylindrical indenter's sharp edges behave like Vickers indenter (as seen in figure 49) which results in exceeding of the elastic regime by small forces

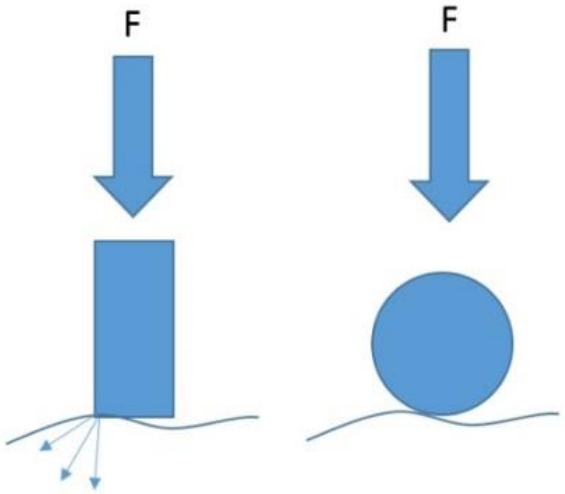

Figure 49 Effects of cylindrical and spherical indenter for uneven surface.

Large diameter spherical indenter let us measure hardness and examine mechanical behaviour near crack zone . The spherical indenter is able to determine mechanical behaviour of a large area without cutting and preparation of the sample. We used one of the real(operational loading) sample to prove the capability of the spherical indenter. The sample in figure 50 is already tested by Vickers from the top of the surface. This time, spherical indenter was used for smooth zone (which is already measured by Vickers) and crack zone which can be seen figure 3

Figure 50 Sample was tested 2 points from different zones: smooth zone crack zone

Loading of 2000 N was applied in the both crack zone and smooth zone by using 5mm spherical indenter and results were compared. Figure 51 presents the typical spherical indentation graph which can give describe mechanical behavior by chosen zone without grinding and cutting of the samples. When comparing with typical spherical indentation graphs, this figure looks accurate even in the crack zone. It means that it is possible to measure directly from any surface. A mathematical approach to determine mechanical behaviour with spherical indenter will be introduced in next chapter.

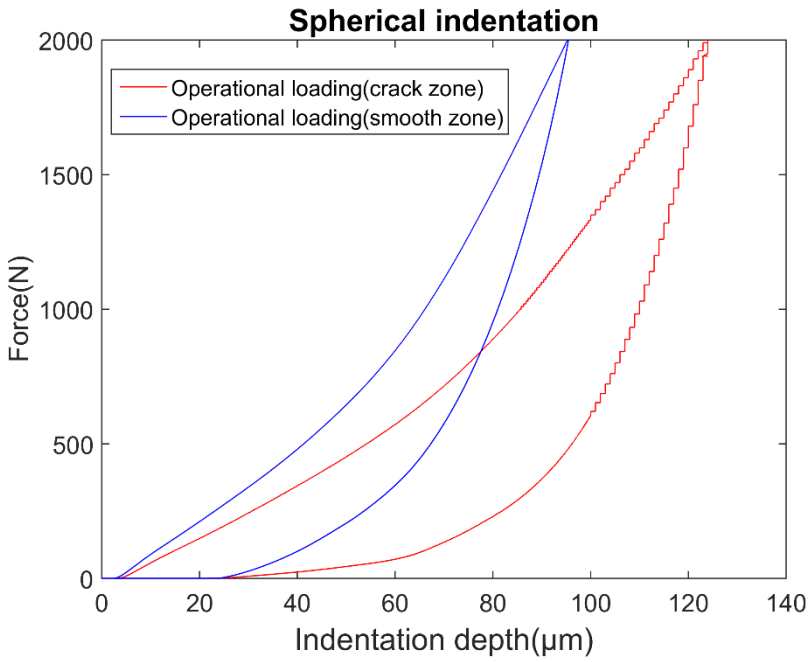

Figure 51 Force-Indentation depth graph for 2 different zones.

7.3.2 Spherical Indentation to determine Mechanıcal Properties of Hadfield's Steel

A number of investigators have proposed methods to measure the yield strength of metals using instrumented indentation experiments performed with a sphere. Brinell was one of the investigators who brings simple approach for indentation method in 1990. It was the first widely used and standardized hardness test in engineering and metallurgy. Indentation diameter is measured by the optical system. However, indentation diameter can't be easily determined because of piling up (pile-up) or sinking in (sink-in) caused by the plastic flow of the material surrounding the ball indenter as seen in figure 52.

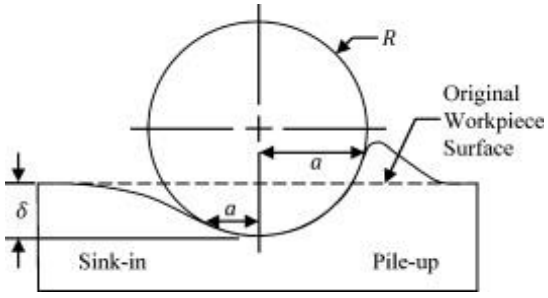

Figure 52. Indentation diameter affected by pile-up or sink-in effect [64].

Brinell hardness can be calculated as;

HBW is calculated in both standards using the SI units as

$$\mathrm{HBW} = 0.102\frac{2F}{\pi D\left(D-\sqrt{D^2-d^2}\right)}$$

Where:

F = applied force (N)

D = diameter of indenter (mm)

d = diameter of indentation (mm)

Application of instrumented indentation methods enables the evaluation based on loading force/ indentation depth, even the study of material response at a particular stage of loading. Typical spherical indentation depth and force graph can be seen in Figure 53. Curve's deflection between indentation (blue), and relaxation curve (red) was examined for several samples. These deflections seem to be more narrow(cover less area) for hardened sample. However, it is more expanded behavior for unhardened samples (as seen in Figure 55), because increasing rate of indentation depth corresponding to the force is more compared to hardened sample. The mathematical expression of deflection can be calculated with equations below. Each P value determines the variation of indentation depth corresponding to the force. We named curve energy deflection change as ''P_{mean} value''.

$P_1 = X_2 - X_1$ (P_2, P_3, P_4, ... P_N can be calculated as P1) (1)

$$P_{mean} = \frac{P_1+P_2+P_3+P_4+\cdots\ldots+P_N}{N} \quad (2)$$

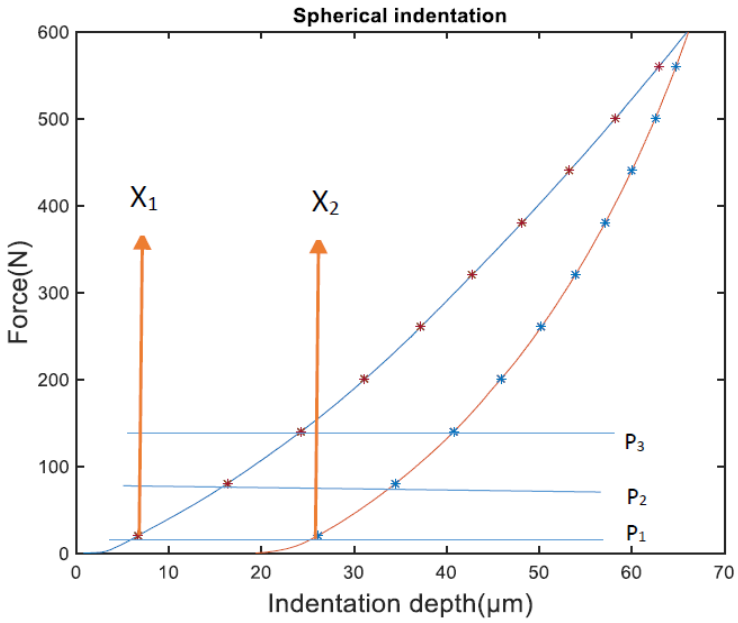

Figure 53 Mathematical calculation of deflection between indentation and relaxation curve

We applied 2000 N for 4 different samples by using 5 mm indenter. After the removal of the indentation force, the diameter of the indentation was measured. Optical-observed contact diameter is influenced by mentioned undesirable effects in figure 52, so at least 5 measurements should be performed in every position. Effect of explosion hardening changes both "Brinell hardness" and "**P_{mean}**" values. There is a reverse ratio between P_{mean} and hardening effect as in Table 6. The harder surface has a narrow graph, low Pmean values, and high Brinell hardness (as expected in Figure 55 and Table 6)

Table 6 Effect of explosion hardening expressed by used mathematical parameters

Samples	**Force (N)**	**P_{mean}**	**Contact diameter (μm)**	**Brinell ardness (N/mm^2)**
After explosive hardening	2000N	22.16	984	274
Before explosive hardening	2000N	36.16	1213	165
Real switch sample - surface	2000N	21.93	907	313
Real switch sample - middle	2000N	36.92	1200	177

7.3.4 Comparison of operational vs. experimental loading effect

To validate the experimental loading system the indentation measurements were performed in the next positions in figure 54:

- Real rail sample (after operational loading) beyond the effect of contact loading,
- The surface area of the real rail sample (after operational and explosive hardening)
- The surface area of the samples with and without explosive hardening (after applied rolling contact test in the laboratory).

The explosive hardened surface of rail samples presented the state of dislocation hardening due to rolling-contact and shock hardening process.

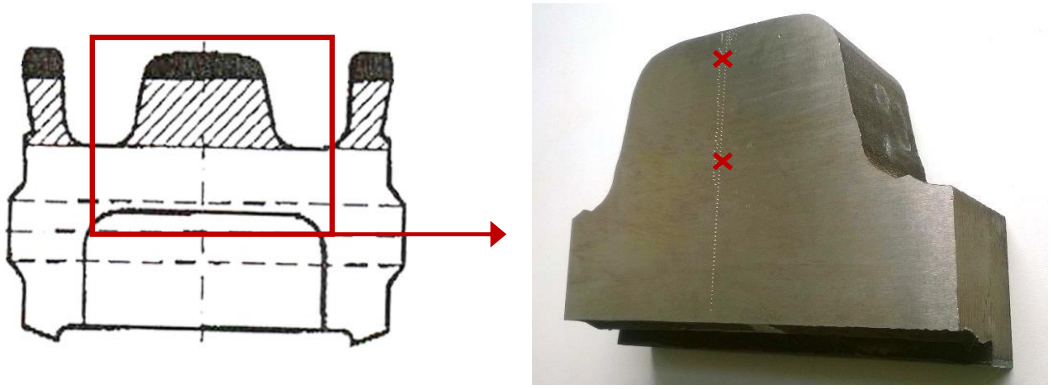

Figure 54 Measurement positions for the real rail sample

Because of the hardening effect of rolling contact and explosive hardening, explosive hardened sample (also after experimental loading) displays almost the same mechanical behavior as the real rail sample (measured near the surface). We calculate P_{mean} values as $\mathbf{P_{Realrailsurface}}$=21.93**,** $\mathbf{P_{Afterexphard}}$=22.16. These values are unsurprisingly very close and their tendency of curve is narrow compared with unhardened samples (figure 55.)

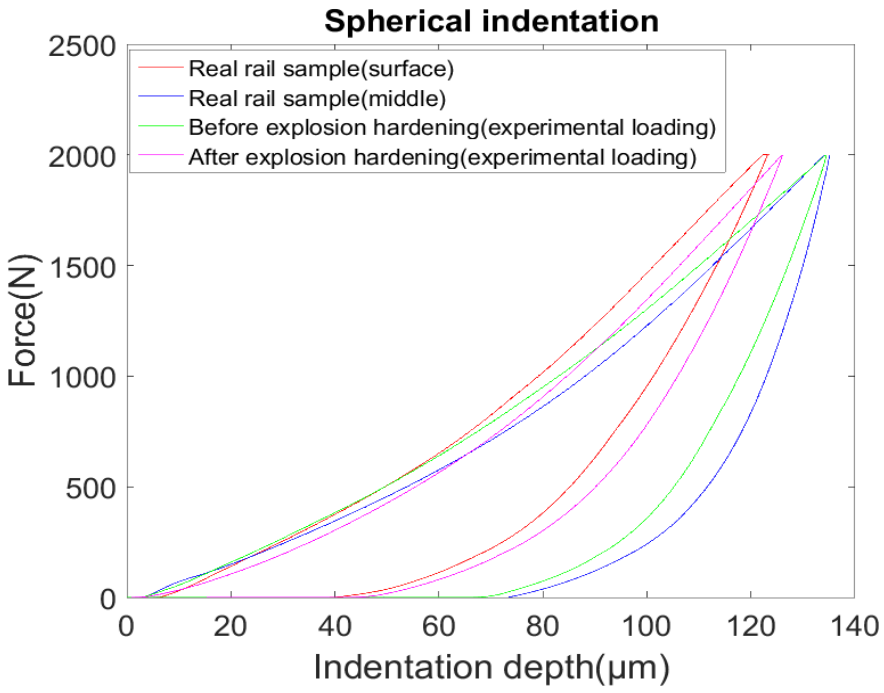

Figure 55 Comparison of indentation curves tendency

We also compared samples without explosion hardening (experimental loading) and real rail sample(middle point).These samples are less affected by operation loading and explosive

hardening.For this reason, curves of these samples have more expanded tendency compared with hardened samples. This curve behavior can be explained by means of P_{mean} values ($\mathbf{P_{Beforeexphard}}$=36.16 , $\mathbf{P_{Realrailmiddle}}$=36.92). These samples display almost the same mechanical behavior.

Experimentally loaded samples in the both stages (with and without explosive hardening) were also measured by suggested method. Loading force-indentation depth graphs were examined and curve tendency was expressed by the simple mathematic method. Effect of hardening was compared between each sample and expected results were also verified by "P_{mean}" value.

8 RESULTS AND DISCUSSION

Results and evaluation methods will lead our further research. In this thesis, degradation progress, mechanical behavior of both Hadfield and pearlitic steel grades are compared and detailed with sort of experiments. Elastic- Plastic response of Hadfield steel was defined both with and without explosion hardening situations.

Following methodology were used to fulfill the specified goals of research:

Simulation of rolling contact process by rolling stand;

The structural and mechanical behavior were tested with special rolling contact machine which is available in the research center. The similar test stand was also used research [65], [66]. The purpose of using this stand is applying real operational contact in laboratory prepared samples. Both Hadfield and pearlitic steel grade tested under load parameters

Loading parameters:

Contact pressure Pmax= 1140MPa
Relative longitudinal slip s = 1%
Revolutions: 400rpm (at the beginning of the experiment)

Surface hardening, depth of the plastic zone, character and depth of the surface damage and wear rate are calculated and compared both Hadfield and pearlitic grade. This way let us understand and determine mechanical behavior of steel under real operational loading.

Metallography analyses of the surface layers for description:

After calculating wear rate under rolling contact test. It is essential to apply metallographic analyses. Metallographic analyses let us obtaining predominant degradation process, depth of the induced structural changes and character and depth of surface damage.

Near- surface dislocations, crack initiation types and direction were observed for both pearlitic and Hadfield steel grade. “White Etching Layers” (WEL) is one of the mechanisms of surface microcracks initialization were involved in the wear during the rolling contact and

typically formed in pearlitic railway steels which were observed several studies [67], [68], [69], [70] In this thesis, WEL and near surface dislocations are introduced by metallographic analysis.

Indentation measurement with 3 types of indenters

Indentation test is necessary for the monitoring of the force and indentation depth relation and hardness value of the material. In this thesis, Vickers, spherical and cylindrical indenter was used. In addition to optical hardness measurement, the test procedure can be force or displacement controlled and the test force F, and indentation depth h was recorded during the experiment.

We firstly used standard Vickers indentation for samples; before rolling contact (with, without explosion hardening), after rolling contact (with, without explosion hardening) All results are recorded. Besides that, Vickers indenter was used for depth of hardening evaluation. The depth of contact–fatigue strengthening was necessary to determine for reliable measurements of surface layer state. But this method sometimes inefficient because surface hardening occurs very small area near surface because of that we use cylindrical indentation method for second stages

In the second stage, comparative yield stress CYS [N/mm^2] was determined by using 1.2 mm cylindrical indenter which was applied to obtain indentation depth corresponding to linear force. The Same attitude was used in article [71] All results are recorded for situations(Before rolling contact after explosive hardening, Before rolling contact without explosive hardening, After rolling contact after explosive hardening, After rolling contact without explosive hardening) Force- indentation depth curves that we obtain displays similar tendency in article [70] Unlike spherical indenter ,cylindrical indenter's sharp edges behave like Vickers indenter which results in exceeding of the elastic regime by small forces. Because of that, we started new measurement with a spherical indenter.

In third stages, mechanical behavior of Hadfield steel obtained by using large diameter spherical indenter. Unlike pointed indenters, elastic-plastic, and fully developed plasticity regime of material can be determined by spherical method because spheres possess the unique ability to transition through perfectly elastic to fully developed plasticity zone. Besides that, large diameter spherical indenter let us measure hardness and examine mechanical behaviour near

crack zone. The spherical indenter is able to determine mechanical behaviour without cutting and high preparation of the sample [73]. Spherical indenter lets us determine large area plastic flow and depth hardening. Unlike cylindrical indenter, plastic strain distributed uniformly under spherical indentation . This situation was explained by fem analysis in the article [71], [72] .

The deformation hardening effect expressed by representative stress-strain curves differs from the values obtained from true stress-strain curves at equivalent strain interval. This is due to the nature of Tabor's formulae, which average the large volume of strained material with the different level of actual hardening [74].Because of that ,new mathematical approaches introduced to find out elastic-plastic response for both cylindrical in spherical indenters.

This work leads us to solve a problem with the determination of mechanical changes in surface layers of railway steels, induced by contact-fatigue loading. In other words, the possibility of suggested way eases monitoring of the elastic-plastic response of the surface. All types of indenter are compared according to the area of usage and their limitations and capabilities are detailed. All evaluation methods can be used as a comparative method for estimation of the residual plastic capacity of the steel. The introduced way of evaluation can be used also as a validation of experimental simulation of the both processes – load fatigue and explosive hardening.

CONCLUSIONS

Dissertation work is devoted to a problem with the determination of mechanical changes in surface layers of railway steels, induced by contact-fatigue loading. This study presents the current types of used rail steels and acting degradation mechanisms as a source of typical material degradation. The main problem for intended research is introduced on the base of the current restrictions for a description of processes acting in thin surface layers.

This study presents degradation progress under operational and experimental loading for pearlitic and Hadfield steel grades. Common casting defects and limitations of both types of steels were explained by metallographic analyses. After examination limitations due to operational loading, Experiments were applied by special rolling contact test machine. All experimental result including metallographic analyses were compared for both Hadfield and pearlitic steel.

This study aims also initial experimental evaluation of the mechanical behaviour of Hadfield steel under several circumstances as explosive hardened vs. unhardened stage. Several types of indentation test were performed to find out the possibilities and restrictions of each considered way for evaluation of processes, induced in surface layers. The initial measurement was performed to understand the elastic-plastic response of Hadfield steel. Different approximations were shown to find out comparative yield stress CYS [N/mm^2].

Examination of degradation progress for surface and sublayers, cylindrical and Vickers and spherical indenter were used. Each of them has advantages depending on usage area experimentally loaded samples in the both stages (with and without explosive hardening) were also measured by suggested methods. Spherical measurement shows that it is possible to apply direct measurement with rough surfaces. New mathematical approaches introduced to find out elastic-plastic response for both cylindrical in spherical indenters.

The comparison of the results has shown the possibility of suggested way for easy monitoring of the elastic-plastic response of the surface. This evaluation can be used as a comparative method for estimation of the residual plastic capacity of the steel. The introduced way of evaluation can be used also as a validation of experimental simulation of the both processes – load fatigue and explosive hardening.

BIBLIOGRAPHY

[1]. Shabana, Ahmed A., et al. "Development of elastic force model for wheel/rail contact problems." *Journal of sound and vibration* 269.1 (2004): 295-325.

[2]. F. Carter, On the action of a locomotive driving wheel, Proc. R. Soc. London 112 (1926) 151–157.

[3]. K. Johnson, Contact Mechanics, Cambridge University Press, Cambridge,1985.

[4]. J. Kalker, Three-Dimensional Elastic Bodies in Rolling Contact, Kluwer Academis Publishers, Dordrecht, 1990.

[5]. X. Zhao, Z. Li, The solution of frictional wheel-rail rolling contact with a 3D transient finite element model: Validation and error analysis, Wear 271 (1-2) (2011) 444–452.

[6]. Hertz, H. R., 1882, Ueber die Beruehrung elastischer Koerper (On Contact Between Elastic Bodies), in Gesammelte Werke (Collected Works), Vol. 1, Leipzig, Germany, 1895.

[7]. D.I. Fletcher, S. Lewis, Creep curve measurement to support wear and adhesion modelling, using a continuously variable creep twin disc machine, Wear. 298-299 (2013) 57–65.

[8]. S.R. Lewis, Measurement, Control and Enhancement of Friction/Traction in a Simulated Wheel/Rail Contact, Doctoral thesis, University of Sheffield, 2011.

[9]. Cooper, P.R. and McEwen, I.J. (1976), "The development of Sandite – a liquid-sand adhesion improver", BR Research Report Ref: TM-TRIB-14(A)

[10]. AWG Adhesion Working Group (2009), "Managing low adhesion", 4th Ed.,www.awg-rail.co.uk.

[11]. Popovici, Radu Ionut. *Friction in wheel-rail contacts*. University of Twente, 2010.

[12]. Bogdanski S, Olzak M, Stupnitzki. Numerical stress analysis of rail rolling contact fatigue cracks. J Wear 1996;191:14–24.

[13]. Cannon DF, Edel D-O, Grassie SL, Sawley K. Rail defects: an overview. Fatigue Fract Eng Mater Struct 2003; 26:865–87.

[14]. Wen Z, Wu L, Li W, Jin X, Zhu M. Three-dimensional elastic–plastic stress analysis of wheel–rail rolling contact. Wear 2011; 271:426–36.

[15]. Bhushan, Bharat. Modern Tribology Handbook, Two Volume Set. Crc Press, 2000.

[16]. Voltr, P., M. Lata, and O. Černý. "Measuring of wheel–rail adhesion characteristics at a test stand." Engineering Mechanics (2012): 181..

[17]. Lewis, R., and R. S. Dwyer-Joyce. "Wear at the wheel/rail interface when sanding is used to increase adhesion." Proceedings of the Institution of Mechanical Engineers, Part F: Journal of Rail and Rapid Transit 220.1 (2006): 29-41.

[18]. Zelin, Michael. "Microstructure evolution in pearlitic steels during wire drawing."*Acta Materialia* 50.17 (2002): 4431-4447.

[19]. P. Clayton, "Predicting the wear of rails on curves from laboratory data." Wear 181 (1995): 11-19.

[20]. Modi, O. P., et al. "Effect of interlamellar spacing on the mechanical properties of 0.65% C steel." *Materials Characterization* 46.5 (2001): 347-352.

[21]. P. Clayton and D. Danks, Effect of interlamellar spacing on the wear resistance of eutectoid steels under rolling-sliding conditions, Wear, 135 (1990) 369-389.

[22]. Alpas, A. T., et al. "The mechanical properties of laminated microscale composites of Al/Al2O3." *Journal of Materials Science* 25.3 (1990): 1603-1609.

[23]. Lindsley, Bruce. "Effects of Cooling Rate on the Hardenability of Chromium Containing P/M Steels."

Advances in Powder Metallurgy & Particulate Materials (2004): 62.
[24]. P. J. Mutton. The influence of microstructure of the wear behavior of rail and wheel materials. M.app.sc. thesis, University of Melbourne, 1985.
[25]. R. Devanathan and P. Clayton. Rolling-sliding wear of three Bainitic steels. Wear, 151:255–267, 1991.
[26]. J. E. Garnham and J. H. Beynon. Dry rolling-sliding wear of Bainitic and Pearlitic steels. Wear, 157:81–109, 1992.
[27]. L. He, The work hardening mechanism of Hadfield steel and it's alloying. Ph.D. Thesis, Xi'an Jiaotong University, Xi'an, 2002, pp. 1–9
[28]. Dastur, Y. N., and W. C. Leslie. "Mechanism of work hardening in Hadfield manganese steel." Metallurgical transactions A 12.5 (1981): 749-759.
[29]. Bowman, Keith, J.: Mechanical behavior of materials. Hoboken, NJ: John Wiley, 2004, xi, 334 p. ISBN 0471241989.
[30]. Zhang, F. C., et al. "Explosion hardening of Hadfield steel crossing." *Materials Science and Technology* 26.2 (2010): 223-229.
[31]. Norman: 'Method of hardening manganese steel', US patent no. 2703297, 1955
[32]. Havlícek, Petr, and Petr Nesvadba. "Application of explosive hardening on railway infrastructure parts." Metal 2011 Conference proceedings. 2011.
[33]. O.D. Sherby, P.E. Armstrong, Metall. Trans. 2 (1971) 3479.
[34]. T.R.G. Kutty, C. Ganguly, D.H. Sastry, Scripta Mater. 34 (1996) 291
[35]. A.G. Evans, E.A. Charles, J. Am. Ceram. Soc. 59 (1976) 371.
[36]. G.R. Anstis, P. Chantikul, D.B. Marshall, B.R. Lawn, J. Am. Ceram. Soc. 64 (1981) 533
[37]. Y.Y. Lim, M.M. Chaudhri, J. Mater. Res. 14 (1999) 2314.
[38]. Cheng L, Xia X, Yu W, et al. Flat-punch indentation of viscoelastic material. J Polym Sci B Polym Phys 2000;38:10.
[39]. VanLandingham MR, Villarrubia JS, Guthrie WF, et al. Nanoindentation of polymers. An overview. Macromol Symp 2001;167:15.
[40]. Lu H, Wang B, Ma J, et al. Measurement of creep compliance of solid polymers by nanoindentation. Mech Time-Depend Mater 2003;7:189.
[41]. Oyen ML, Cook RFJ. Load–displacement behavior during sharp indentation of viscous–elastic–plastic materials. Mater Res 2003;18:139.
[42]. Zhang CY, Zhang YW, Zeng KY. Extracting the mechanical properties of a viscoelastic polymeric film on a hard elastic substrate. J Mater Res 2004;19:3053.
[43]. Sakai M, Zhang J, Matsuda A. Elastic deformation of coating/ substrate composites in axisymmetric indentation. J Mater Res 2005;20:2173.
[44]. Odegard GM, Gates TS, Herring HM. Characterization of viscoelastic properties of polymeric materials through nanoindentation. Exp Mech 2005;45:130.
[45]. Huang G, Lu HB. Measurement of Young's relaxation modulus using nanoindentation. Mech Time-Depend Mater 2006;10:229.
[46]. Ozkan N, Xin H, Chen XD. Application of a depth sensing indentation hardness test to evaluate the mechanical properties of food materials. J Food Sci 2002;67:1814.

[47]. Rho JY, Tsui TY, Pharr GM. Elastic properties of human cortical and trabecular lamellar bone measured by nanoindentation. Biomaterials 1997;18:1325.

[48]. Moses DN, Mattoni MA, Slack NL, et al. Role of melanin in mechanical properties of Glycera jaws. Acta Biomater 2006;2:521.

[49]. Angker L, Swain MV. Nanoindentation: application to dental hard tissue investigations. J Mater Res 2006;21:1893.

[50]. Ebenstein DM, Pruitt LA. Nanoindentation of biological materials. Nano Today 2006;1:26.

[51]. Oyen ML, Ko CC. Examination of local variations in viscous, elastic, and plastic indentation responses in healing bone. J Mater Sci Mater Med 2007;18:623.

[52]. Yang S, Saif MTA. Force response and actin remodeling (agglomeration) in fibroblasts due to lateral indentation. Acta Biomater 2007;3:77.

[53]. Hill R, Storakers B, Zdunek AB. A theoretical study of the Brinell hardness test. Proceedings of the Royal Society of London1989;423:301–30.

[54]. Biwa S, Storakers B. An analysis of fully plastic Brinell indentation. Journal of Mechanics and Physics of Solids 1995;43:1303–33.

[55]. Field JS, Swain MV. Determining the mechanical properties of small volumes of material from submicrometer spherical indentations. Journal of Materials Research 1995;10(1):101–12.

[56]. Adler TA, Dogan ON. Damage by indentation and single impact of hard particles on a high chromium white cast iron. Wear 1997;203–204:257–66.

[57]. Taljat B, Zacharia T, Kosel F. New analytical procedure to determine stress–strain curve from spherical indentation data. International Journal of Solids and Structures 1998;35:4411–

[58]. Kucharski S, Mro´ z Z. Identification of plastic hardening parameters of metals from spherical indentation tests. Materials Science & Engineering A 2001;318(1–2):65–76.

[59]. Kucharski S, Mro´ z Z. Identification of hardening parameters of metals from spherical indentation test. Journal of Engineering Materials and Technology—Transactions of the ASME 2001;123:245–50.

[60]. Huber N, Tsakmakis Ch. A finite element analysis of the effect of hardening rules on the indentation test. Journal of Engineering Materials and Technology—Transactions of the ASME 1998;120:143–8.

[61]. R.L. Smith & G.E. Sandland, "An Accurate Method of Determining the Hardness of Metals, with Particular Reference to Those of a High Degree of Hardness," *Proceedings of the Institution of Mechanical Engineers*, Vol. I, 1922, p 623–641.

[62]. Bowman, Keith, J.: Mechanical behavior of materials. Hoboken, NJ: John Wiley, 2004, xi, 334 p. ISBN 0471241989.

[63]. R. Devanathan and P. Clayton. Rolling-sliding wear of three Bainitic steels. Wear, 151:255–267, 1991.

[64]. ANDERSON DD, WARKENTIN AA, BAUER RR. Simulation of Deep Spherical Indentation Using Eulerian Finite Element Methods. ASME. J. Tribol.2011; 133(2):021401-021401-8. doi:10.1115/1.4003703.

[65]. Eadie, Donald T., et al. "The effects of top of rail friction modifier on wear and rolling contact fatigue: Full-scale rail–wheel test rig evaluation, analysis and modelling." Wear 265.9 (2008): 1222-1230.

[66]. Cannon, D. F., and H. Pradier. "Rail rolling contact fatigue research by the European Rail Research

Institute." Wear 191.1 (1996): 1-13.

[67]. Newcomb, S. B., and W. M. Stobbs. "A transmission electron microscopy study of the white-etching layer on a rail head." Materials Science and Engineering 66.2 (1984): 195-204.

[68]. Zhang, H. W., et al. "Microstructural investigation of white etching layer on pearlite steel rail." Materials Science and Engineering: A 421.1 (2006): 191-199.

[69]. Carroll, R. I., and J. H. Beynon. "Rolling contact fatigue of white etching layer: Part 1: Crack morphology." Wear 262.9 (2007): 1253-1266

[70]. Seo, JungWon, et al. "Numerical stress analysis and rolling contact fatigue of White Etching Layer on rail steel." International Journal of Fatigue 33.2 (2011): 203-211.

[71]. Lu, Y. Charles, Siva NVRK Kurapati, and Fuqian Yang. "Finite element analysis of cylindrical indentation for determining plastic properties of materials in small volumes." Journal of Physics D: Applied Physics 41.11 (2008): 115415.

[72]. Schmidová E., Bozkurt F., Scmid m., Culek B., local elastıc plastıc reponse of welding joints of domex steel in metal 2016. Ostrava: TANGER, pp 104 ISBN 978-80-87294-66-6.

[73]. J.Cech, P Housdil, O. Kovarnik., M. Skeren, “Effect of Actual Indenter Shape on the Resultsof Spherical Nanoindentation” , *Defect & Diffusion Forum* 2016 *Vol. 368, pp 11-14, ISSN: 1662-9507,*

[74]. Haušild, P., Materna, a., Nohava, J. On the identification of stress-strain relation by instrumented indentation with spherical indenter, *Mater.Design* 37, 2015, pp.373-378.

PUBLICATIONS OF THE PHD STUDENT RELATED TO THE THEME OF THE DISSERTATION

[75]. Kaya, Utku, "The elastic-plastic response of Hadfield steel under indentation test" *Series B Jan Perner Transport Faculty* (2015): p33.

[76]. Schmidová, E. - Culek, B. - Kaya, U., Effect of Rolling Contact Fatigue on the Elastic-Plastic Response of Hadfield steel. in metal 2015. ostrava: tanger, spol. s r.o., 2015. s. 101-107. ISBN 978-80-87294-58-1.

[77]. Kaya U., Schmidová E., "Spherıcal Indentatıon Approach to Determıne Mechanıcal Properties of Hadfield's steel" In METAL 2016. Ostrava: TANGER, pp 104 ISBN 978-80-87294-66-6.

[78]. Schmidová E. , Kaya, U., Schmid M., Culek B., "Rolling-Contact Hardening Evaluated by Indentation" , *Defect & Diffusion Forum* 2016 *Vol. 368, pp 11-14, ISSN: 1662-9507,*

[79]. Kaya U., Schmidova E., "Matematical Apparoach for Spherical Indentation Curve of Hadfield's Steel", Advanced Manufacturing and Repair Technologies in Vehicle Industry May 25 – 27, 2016 Western Tatras - Zuberec, Slovakia